N A T U R A L   R E S O U R C E S

GEOLOGIC MAPPING AND GEOTHERMAL ASSESSMENT OF THE WIND RIVER VALLEY, SKAMANIA COUNTY, WASHINGTON

by Jessica L. Czajkowski, Jeffrey D. Bowman,
Logan A. Fusso, and Darrick E. Boschmann

WASHINGTON
DIVISION OF GEOLOGY
AND EARTH RESOURCES

Open File Report 2014-01
March 2014

WASHINGTON STATE DEPARTMENT OF
Natural Resources
Peter Goldmark - Commissioner of Public Lands

GEOLOGIC MAPPING AND GEOTHERMAL ASSESSMENT OF THE WIND RIVER VALLEY, SKAMANIA COUNTY, WASHINGTON

by Jessica L. Czajkowski, Jeffrey D. Bowman,
Logan A. Fusso, and Darrick E. Boschmann

WASHINGTON
DIVISION OF GEOLOGY
AND EARTH RESOURCES

Open File Report 2014-01
March 2014

WASHINGTON STATE DEPARTMENT OF
Natural Resources
Peter Goldmark - Commissioner of Public Lands

Washington State Department of Natural Resources
Division of Geology and Earth Resources

Mailing Address:	*Street Address:*
MS 47007	Natural Resources Bldg, Rm 148
Olympia, WA 98504-7007	1111 Washington St SE
	Olympia, WA 98501

*Phone:*360-902-1450; *Fax:* 360-902-1785
E-mail: geology@dnr.wa.gov
Website: http://www.dnr.wa.gov/geology

Publications List:
http://www.dnr.wa.gov/ResearchScience/Topics/GeologyPublicationsLibrary/Pages/pubs.aspx

Washington Geology Library Searchable Catalog:
http://www.dnr.wa.gov/ResearchScience/Topics/GeologyPublicationsLibrary/Pages/washbib.aspx

Washington State Geologic Information Portal:
http://www.dnr.wa.gov/geologyportal

Suggested Citation: Czajkowski, J. L.; Bowman, J. D.; Fusso, L. A.; Boschmann, D. E., 2014, Geologic mapping and geothermal assessment of the Wind River valley, Skamania County, Washington: Washington Division of Geology and Earth Resources Open File Report 2014-01, 30 p., 1 pl., scale 1:24,000.

Published in the United States of America

Table of Contents

FIGURES

TABLES

PLATE

Geologic Mapping and Geothermal Assessment of the Wind River Valley, Skamania County, Washington

by Jessica L. Czajkowski, Jeffrey D. Bowman, Logan A. Fusso, and Darrick E. Boschmann
Washington Division of Geology and Earth Resources
MS 47007; Olympia, WA 98504-7007

INTRODUCTION

The Wind River valley, a northwest-trending valley draining southeastward into the Columbia River Gorge near Washington's southern border (Fig. 1), is a subject of interest in geothermal exploration. There are numerous thermal and mineral springs and seeps along and adjacent to this valley, several of which are now or were previously developed into resorts, such as Bonneville and St. Martins (Carson) Hot Springs. Temperatures measured in several temperature-gradient boreholes drilled in the early 1980s revealed elevated gradients within this valley. In addition, several water wells at the southern end of the valley, near the town of Carson, contain warm water. Based on the presence of thermal and mineral springs, relatively young intrusives, and warmer water along the valley's axis, some workers postulate that a valley-parallel structure channels high heat flow from cooling intrusives at depth within and along the length of this valley.

The Washington Department of Natural Resources (WADNR), Division of Geology and Earth Resources (DGER), has recently conducted a geothermal data compilation program within Washington State, including the Wind River valley. This work was funded by federal grants from both the U.S. Department of Energy and U.S. Forest Service and includes geologic mapping, thermal and mineral spring water chemistry analyses, temperature-gradient logging in existing wells, and drilling several temperature-gradient holes as much as 700 feet deep. One of these boreholes is located in the upper Wind River valley, near Tyee Springs (Fig. 1; Plate). The borehole site was chosen because of its proximity to several springs, postulated faults, earthquake hypocenters, and aeromagnetic anomalies. Another consideration was a lack of gradient data; higher gradients have already been established in the lower reaches of the valley.

Recent multi-criteria modeling using GIS (Boschmann and others, unpub. data) generated a statewide geothermal favorability model. This model is the weighted sum of rasterized data, including geothermal gradients; proximity to young, siliceous igneous intrusives and volcanic vents; proximity to faults, fault intersections, and earthquakes; distance to transmission lines; and elevation. The model was created to estimate the relative favorability of locating and developing geothermal resources. One of the most favorable areas indicated by the model is the Wind River valley (Fig. 1A).

New geologic mapping and geophysical investigation of the Wind River valley were undertaken to better understand the geology, age, and nature of alteration; to obtain structural data; and to improve the accuracy of existing mapping in support of the recently drilled borehole. In addition, several thermal and mineral springs (Fig. 1B) were re-analyzed for major-element chemistry, as well as helium, oxygen, and deuterium isotopes. An accurate assessment of geologic conditions both at the surface and at depth is critical to future development of geothermal resources and is the first step in exploration.

PREVIOUS WORK

The Wind River valley area was first mapped in 1961 by William Wise at 1:62,500-scale and later mapped as part of a reconnaissance-style, geochemistry-based geothermal project at 1:24,000-scale by Berri and Korosec (1983). Mapping for this area was subsequently revised by Korosec (1984) within the Hood River 1:100,000-scale geologic map. Other reconnaissance-scale compilation geologic maps that include this area are Hammond (1980) and Bela (1982).

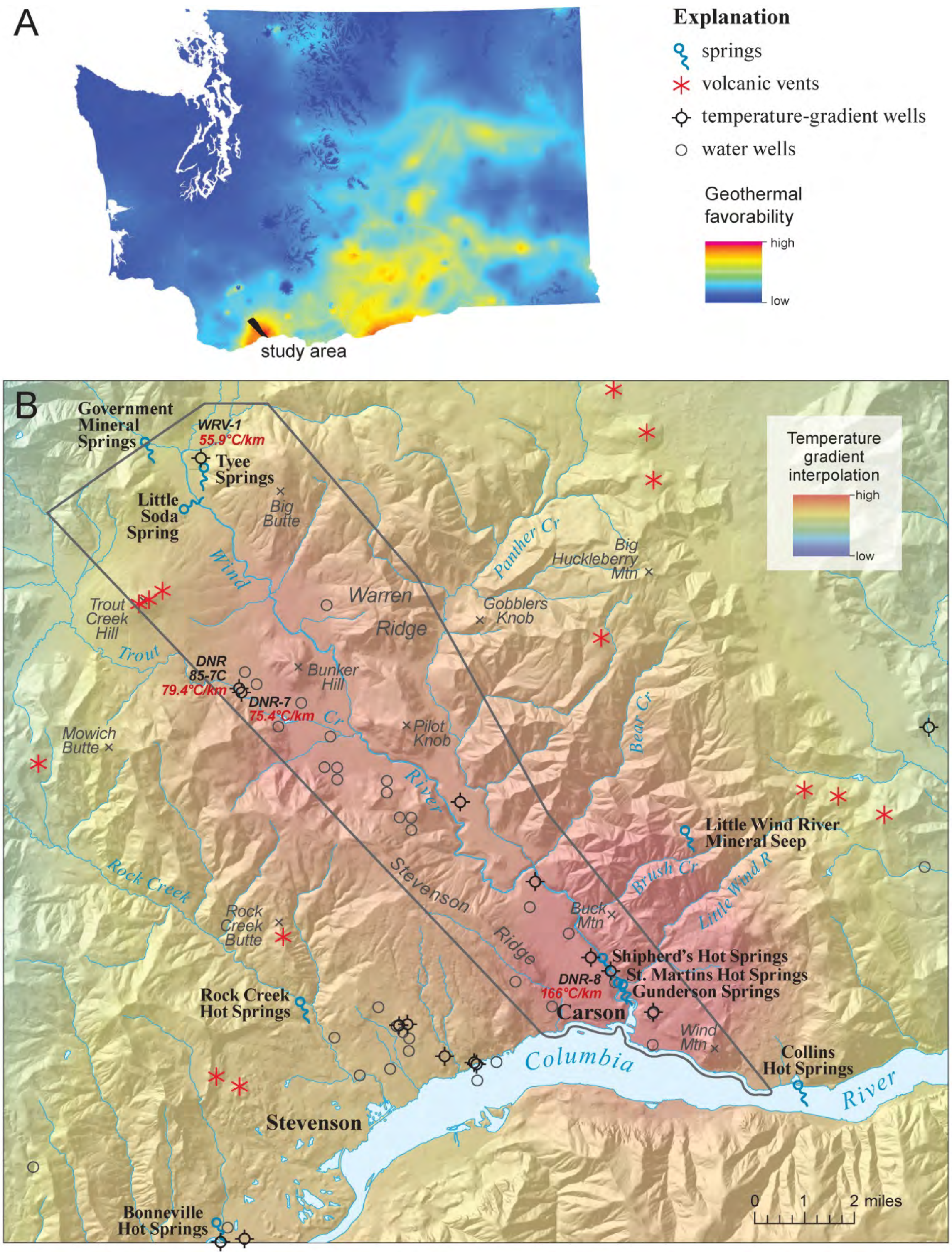

Figure 1. Wind River valley study area**. A.** Relative geothermal favorability map of Washington State showing major stratovolcanoes and study area. Geothermal favorability was assigned based on numerous factors, including elevation, proximity to transmission lines, intrusive rocks, volcanic centers, thermal springs, temperature-gradient wells, and mapped faults and earthquakes (Boschmann and others, DGER, unpub. data, 2013). **B.** Wind River valley and vicinity showing interpolated temperature-gradient, volcanic vents, thermal and mineral springs, temperature-gradient boreholes, and water wells in which temperature was recorded (temperatures not shown).

Spring sampling and temperature monitoring have been conducted repeatedly over the last half century at most of the springs in and around the valley, including Government and Little Wind River Mineral Springs and St. Martins (Carson), Rock Creek, Shipherd's (St. Martin on the Wind), and Bonneville Hot Springs.

In the early 1980s, three temperature-gradient boreholes, DNR-85-7C, DNR-7 (DNR-TRCK), and DNR-8 (DNR-CRSN), were drilled by DGER (Fig. 1). All of these wells yielded elevated gradients; the highest gradient (166°C/km) was near the town of Carson. Several elevated gradients were also measured in nearby water wells.

METHODS

Geologic mapping was performed primarily during the months of June 2012 and July and August of 2013. A series of U.S. Geological Survey 7.5-minute topographic maps was used as a base map, but contact locations were refined by reference to a 10-meter digital elevation model (DEM), 2-foot lidar, aerial photos, and field observations. Access to observation locations was by abandoned or decommissioned Forest Service logging roads, the Pacific Crest Trail, and off-road terrain traverses. Field samples were collected for comparison, further thin-section analysis, and whole rock chemistry. Thin sections were created by Spectrum Petrographics. Whole rock geochemistry was performed by the GeoAnalytical Laboratory of Washington State University. During the 2013 field season, we also performed a series of ground-based magnetic and electrical resistivity surveys along numerous transects throughout the study area (*see* Fig. 3).

Temperature-gradient borehole WRV-1 (Fig. 1) was drilled in early August of 2012 by Schneider Equipment, Inc. Drill cuttings were collected every 10 feet for identification. In preparation for drilling, we also performed a small active-seismic survey at the drill site in an attempt to determine depth to bedrock. Natural gamma and resistivity were measured in the uncased borehole using a Century Geophysical System VI borehole logging tool prior to 2-inch-casing installation and well completion. After well completion and a three- to four-week period of equilibration, temperature-gradient logging was performed on three occasions using a Hobo U12 temperature logger.

Thermal and mineral springs in the area were sampled throughout 2011, 2012, and 2013 for major element analytes, ^{18}O, deuterium, and helium. Major-element chemistry analyses were performed by Sierra Environmental Monitoring Inc.; ^{18}O and deuterium samples were analyzed by Washington State University; and helium samples were analyzed by Scripps Institute of Oceanography at the University of California San Diego.

GEOLOGIC SETTING

Geomorphic Setting

The map area (Fig. 1) lies along the Cascade crest, south of Mount St. Helens, at elevations between ~100 and 3,400 feet above mean sea level. The area contains numerous sharp ridges and broad crests, including Big Butte, Warren Ridge, Pilot Knob, Stevenson Ridge, Buck Mountain, and Wind Mountain. Valleys are typically steep-sided, and the area is heavily forested with old- and second-growth timber. The map area consists of a broad, generally level, alluvial channel in the northern part of the valley, which narrows significantly at its southern end and is likely controlled by adjacent bedrock and overlying volcanic flows beneath the alluvium.

Geologic Overview

The upper Wind River valley is predominantly underlain by shallowly west-dipping, intercalated pyroclastic and volcaniclastic rocks of Eocene to Oligocene age, with the uppermost rocks possibly lower Miocene in age. These rocks were originally called the Weigle formation by Wise (1961), but were later associated with the Ohanapecosh Formation (Wise, 1970; Bela, 1982; Hammond, 1980; Berri and Korosec, 1983; Korosec, 1984). We opted to use the formal 'Ohanapecosh Formation' for this unit for consistency, although we acknowledge that the vent source for the section exposed in the Wind River area is likely different from that of the type section originally described by Fiske and others (1963).

Hypabyssal diorite and gabbro intrusions of late Oligocene to Pliocene age are exposed in numerous locations within the map area, and in many places were observed to alter the regional layering orientation of the overlying Ohanapecosh Formation. In general, emplacement of these intrusives can be associated with abundant alteration and silicification of the Ohanapecosh Formation, especially in the northwest part of the map area. Based on field mapping and the amount of alteration and silicification, we speculate that much of the area is underlain by shallowly

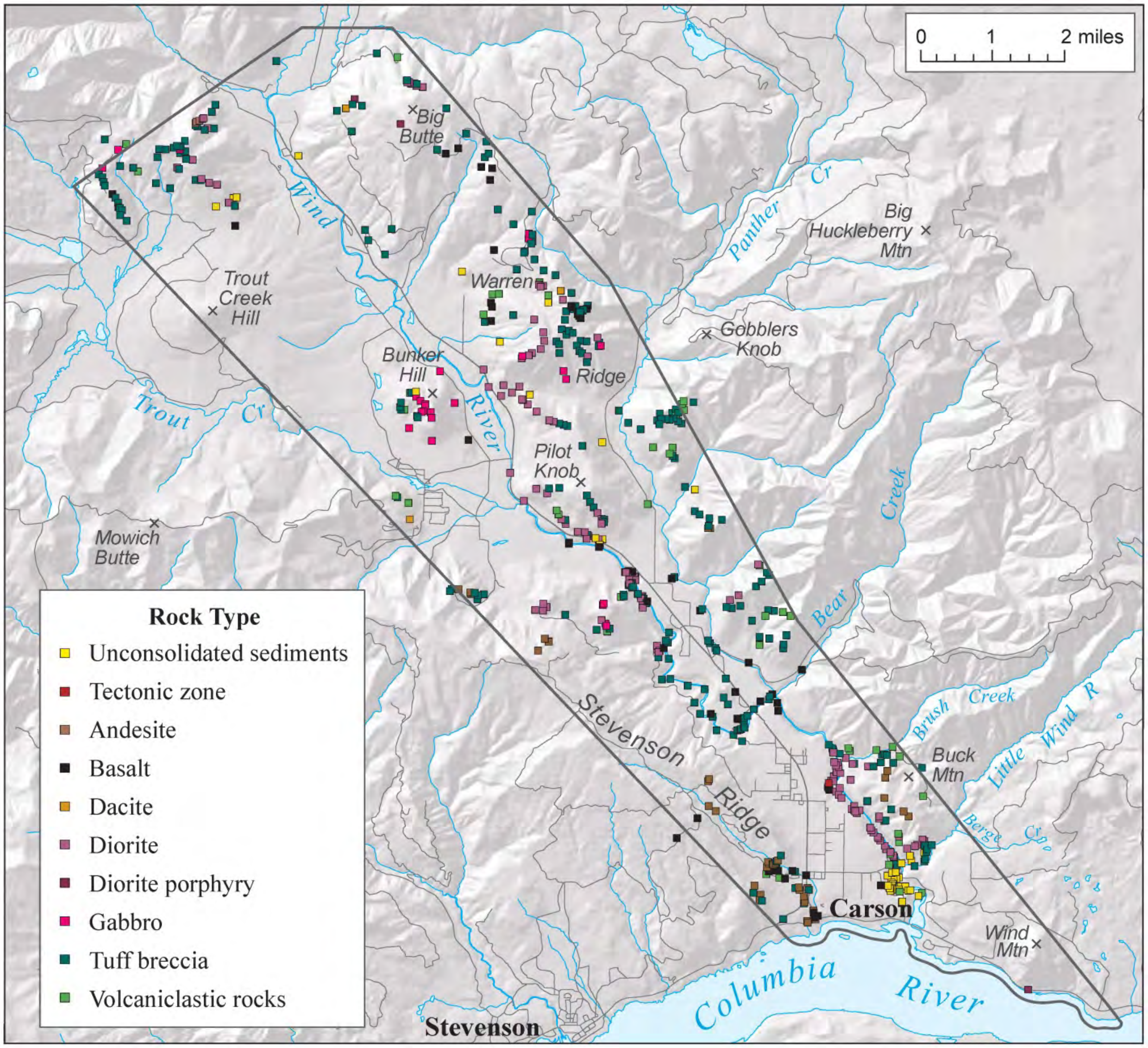

Figure 2. Upper Wind River valley and vicinity showing field observation sites and corresponding rock types.

buried intrusive rocks. Numerous predominantly northeast- and northwest-trending basaltic and andesitic dikes traverse the map area.

In the northeastern part of the map area, two small Miocene basalt/basaltic andesite flows erupted through the Ohanapecosh Formation. The western edge of the map area contains a package of thickly interlayered Miocene lava flows and volcaniclastic rocks that form Stevenson Ridge.

The eastern flank of the Quaternary Trout Creek Hill volcano is in the northwestern third of the map area. The rubbly flows consist of relatively unweathered, scoriaceous, dark gray basalt with abundant labradorite phenocrysts. Exposure of this basalt is poor along the flanks of the volcano. Flows from vents were directed east into the Wind River valley around Bunker Hill and downvalley to the Columbia River.

Quaternary unconsolidated sediments in the field area include rockfall and talus deposits, landslide deposits, colluvium, alluvial fans, and alluvium. These units are mapped, yet are not differentiated.

DESCRIPTION OF MAP UNITS

We sought to show bedrock units; however, we also attempted to note where Quaternary unconsolidated sediments were especially thick and obscured any evidence of underlying bedrock. In some areas, due to poor exposure, we relied considerably on geomorphology, field relations, and subsurface records. See Figure 2 for a map of our field observation sites.

Quaternary Unconsolidated Deposits

Qs **Unconsolidated sediment**—Locally derived deposits including talus, rockfalls, landslides, colluvium, alluvial fans and alluvium; excludes modified land. These units were not studied in any detail and were mapped to note where bedrock was obscured.

Talus deposits flank most steep ridges and are especially prominent below areas underlain by intrusive rocks, such as the north flank of Bunker Hill, the upper south flank of Big Butte, and the south flanks of both Warren Ridge and Pilot Knob (not mapped).

A large rockfall deposit was noted below a cliff of diorite on the southeast flank of Sinter ridge immediately north of the Trout Creek Hill volcano. Across the Wind River valley to the east, the west flank of Big Butte is blanketed by several large landslide deposits, generally situated within west-dipping, slope-parallel volcaniclastic deposits of the Ohanapecosh Formation. Identification of these slides was due in part to hummocky topography, pistol-butt trees, and an uncharacteristic lack of bedrock exposure. Several large landslides were noted to the south in the uplands west of the town of Carson and to the southeast in the neighboring community of Home Valley; all were sited within either the Ohanapecosh Formation or the volcanic rocks of Stevenson Ridge.

Alluvial fans and thick deposits of loose, poorly sorted, angular colluvium obscure bedrock exposures on the lower halves of most ridges and peaks, especially along west-facing slopes where the general bedding attitude of the volcaniclastics parallels that of the slope.

Alluvium deposits composed predominantly of sandy gravel line the lowest portions of the Wind River valley north of Bunker Hill. Near Bunker Hill, well records indicate that these deposits are intercalated with the basalt flow from Trout Creek Hill, which temporarily dammed the river in this area. Little to no alluvium was observed within the Wind River channel south of its intersection with Trout Creek, except within 1.5 river miles of the river mouth. We opted not to map the variably thick alluvium atop the Trout Creek basalt flow (unit Qvb_{tch}) in the southern part of the valley floor, due to poor exposure and lack of well data to confirm mappable thickness.

Quaternary Volcanic Rocks

Qvb_{tch} **Basalt of Trout Creek Hill**—Scoriaceous, dark blackish-gray basalt with phenocrysts (<1 mm) of subhedral labradorite and anhedral olivine within a groundmass containing microlitic euhedral albite and granular pyroxene. Outcrop of this basalt is extremely poor along the flanks of the volcano, but the unit is well exposed in the Wind River channel south of the intersection with Trout Creek where the river has cut through these flows, creating 100- to 200-foot-high cliffs. Geochemistry from samples of the basalt (Plate, map nos. G12 and G17), originally presented in Korosec (1987), is shown on Table 1. Korosec (1984) and Berri and Korosec (1983) reported a K-Ar age of 0.34 ±0.07 Ma for samples from this unit at two locations (Plate, map nos. 1 and 2; Table 2).

Qvb_{ih} **Basalt of Indian Heaven**—Highly vesicular, dark grayish-black basalt. Outcrop of this basalt is not found within the northeast-trending upper Wind River valley northeast of the U.S. Forest Service Fish Hatchery (Plate). However, this flow was encountered in the newly drilled geothermal borehole WRV-1 between 6 and 51 feet. Neighboring well logs indicate that this flow does not extend to the fish hatchery. No direct age has been obtained from this flow, but its maximum age is constrained by the basaltic andesite flows of Juice Creek for which a K-Ar age of 1.4 ±0.06 Ma for was obtained outside the map area by Korosec (1987; 1989).

Pliocene Intrusive Rocks

Rqd_{w} **Quartz diorite porphyry of Wind Mountain**—Light gray, relatively unweathered, porphyritic clinopyroxene quartz diorite forming Wind Mountain in the southeast corner of the map area; typically very fine to fine grained with 1- to 2-mm plagioclase and quartz porphyry, with quartz, plagioclase, apatite, and minor clinopyroxene common in the groundmass; forms irregular colonnades. Phillips and others (1986) and Korosec (1987) report whole-rock K-Ar ages of 4.9 ±0.8 Ma and 6.6 ±0.7 Ma from this unit on the north and south sides of the mountain, respectively (Plate, map nos. 8 and 9; Table 2). A similar age of 5.7 ±0.6 Ma was obtained from a quartz diorite on Shell Rock to the southeast of Wind Mountain across the Columbia River in Oregon (not shown). Geochemistry from a sample of the quartz diorite on Wind Mountain (Plate, map no. G18), originally presented in Korosec (1987), is shown on Table 1.

Miocene to Oligocene Volcanic Rocks

Mvb **Basalt and basaltic andesite**—Dark grayish-black to dark blackish-gray, seriate to porphyritic basalt to basaltic andesite. These small flows have been quarried extensively in the past. Korosec (1987) obtained a whole-rock K-Ar age of 20.8 ±1.2 Ma from a basaltic andesite sample of this unit southeast of Big Butte (Plate, map no. 3; Table 2). Geochemistry from samples of the basalt and basaltic andesite (Plate, map nos. G19, G20, and G21), originally presented in Korosec (1987), is shown on Table 1.

MΦvas
MΦvcs **Volcanic rocks of Stevenson Ridge**—Interlayered sequence of basaltic andesite to andesite flows, flow breccia, tuff, and clay. Andesite is typically porphyritic with abundant plagioclase porphyry and common intergranular orthopyroxene, sericite alteration, concentric zoning, and felty groundmass. Unit is subdivided into predominantly lava flows with minor pyroclastic rocks (unit MΦvas) and predominantly pyroclastic rocks with minor lava flows (unit MΦvcs). The notable differences between the pyroclastic rocks from this unit and the underlying Ohanapecosh Formation are that the clast lithology is mostly basaltic and there is less variability in clast type than with similar rocks of the Ohanapecosh Formation. The upper portions of tuff layers between lava flows are significantly altered to clay and likely provide surfaces on which slope instability occurs. Korosec (1987) obtained a whole-rock K-Ar age of 15.7 ±1.5 Ma from a basaltic andesite sample (Plate, map no. 10; Table 2), although, based on a 23.6 ±1.2 Ma whole-rock K-Ar age from a basalt at Sedum Point (Korosec, 1987; Table 2), it is either a younger unit sitting on top of the Stevenson Ridge lavas or a flow from the unit's upper reaches; the younger age obtained from low in the section is spurious. This unit has been correlated with the basalt of Three Corner Rock to the west (Hammond, 1980; Korosec, 1987; Phillips, 1987; Berri and Korosec, 1983) that Hammond (1980) estimates is late Oligocene to early Miocene in age. Geochemistry for samples of basaltic andesite (Plate, map nos. G13 and G16), originally published in Berri and Korosec (1983), is shown on Table 1.

Miocene to Oligocene Intrusive Rocks

MΦi **Dikes**—Dark gray to black, predominantly aphanitic to fine- to medium-grained hypabyssal rocks of basaltic and andesitic composition, although composition can range to dacite; textures locally range between intrusive and extrusive; locally composite, scoriaceous, and variably weathered. These dikes were either previously unmapped or erroneously mapped as either part of dioritic sills and plugs or as interbedded lava flows within the Ohanapecosh Formation (Wise, 1961, 1970; Berri and Korosec, 1983; Korosec, 1987). Dikes are generally geomorphologically distinct, creating narrow, elongate ridges, and at times can be followed for thousands of feet. We suspect that there are additional dikes in the map area, yet time constraints and poor exposure were prohibitive.

Berri and Korosec (1983) obtained an age of 22.7 ±0.9 Ma from a dacite sample taken 0.6 miles to the southwest of the Stabler-Hemlock (Wind River) Ranger Station (Plate, map no. 4; Table 2). The dacite was tentatively interpreted as an interbedded flow in the Ohanapecosh Formation, and because of its young age, was thought to be thermally reset by heat from nearby diorite emplacement. Berri and Korosec (1983) also noted that the exposures of basalt, basaltic andesite, and dacite flows within the Ohanapecosh Formation could not be traced for any appreciable distance. We suspect that many of these flows are instead dikes or clusters of dikes, as we noted very few demonstrable instances of observable intercalated flows within the Ohanapecosh Formation in the map area. We visited the dacite sampling location shown in Berri and Korosec (1983), which upon first glance, showed geomorphic expression very similar to dikes mapped in the field area. There we noted a 50- to 100-foot-wide ridge of light gray, extremely hard dacite traversing northwestward vertically up a hillside, clearly truncating gently northwest-dipping tuff and tuff breccia beds on either side of it. We have tentatively assigned the 22.7 Ma age instead to dike emplacement, based on this field evidence and the abundance of dikes of variable composition in the area. Geochemistry for several samples (Plate, map nos. G2, G4, G22, and G23) is shown on Table 1.

Table 1. Normalized major element chemistry of igneous rocks in the Wind River map area. Except for sample G1 (this study), data originally presented in Berri and Korosec (1983) and Korosec (1987).

Map no.	Sample ID	Lithology	Unit symbol[1]	SiO_2	TiO_2	Al_2O_3	Fe_2O_3	FeO	MnO	MgO	CaO	Na_2O	K_2O	P_2O_5	Total
G1	WR-15-491	gabbroic diorite	MΦid	55.14	1.036	17.67	– – –	7.73	0.13	5.66	8.50	3.31	0.63	0.178	97.81
G2	2	dacite	MΦi	67.27	0.76	14.09	3.23	3.70	0.16	1.04	2.87	4.36	2.28	0.22	99.98
G3	3	gabbro	MΦigb	53.60	1.35	19.20	4.34	4.98	0.15	3.01	8.01	4.33	0.78	0.24	99.99
G4	4	andesite/ diorite	MΦi	56.56	1.78	16.43	5.10	5.84	0.19	2.61	5.42	4.77	1.02	0.29	100.01
G5	5	diorite	MΦid	56.91	1.92	15.45	4.85	5.56	0.20	2.81	6.20	4.01	1.61	0.48	100.00
G6	6	diorite	MΦid	56.69	1.84	15.86	4.78	5.48	0.19	3.03	5.91	4.15	1.64	0.44	100.01
G7	7	sedimentary rock	ΦEvc$_o$	63.15	1.05	15.62	3.59	4.11	0.18	1.80	5.80	3.10	1.37	0.24	100.01
G8	8	diorite	MΦid	61.77	1.44	14.76	4.42	5.06	0.18	1.48	5.57	3.50	1.37	0.46	100.01
G9	9	diorite	MΦid	55.10	1.81	15.93	5.49	6.28	0.22	3.20	6.42	4.24	0.99	0.32	100.00
G10	10	diorite	MΦid	57.64	1.88	16.40	4.26	4.89	0.17	2.81	5.87	4.29	1.49	0.31	100.01
G11	11	tuff breccia	ΦEvc$_o$	64.30	0.72	14.87	3.02	3.46	0.18	1.17	6.55	2.94	1.76	1.03	100.00
G12	12	basalt	Qvb$_{tch}$	51.09	1.14	17.45	4.74	5.43	0.17	7.19	8.85	3.42	0.35	0.17	100.00
G13	13	basaltic andesite	MΦva$_s$	54.32	1.50	17.72	4.33	4.96	0.16	3.51	8.23	4.01	0.98	0.29	100.01
G14	14	diorite	MΦid	59.41	1.07	16.61	3.47	3.98	0.12	3.65	6.62	3.73	1.10	0.22	99.98
G15	15	diorite	MΦid	59.07	0.92	17.47	3.19	3.66	0.11	3.80	6.45	4.02	1.14	0.16	99.99
G16	16	basaltic andesite	MΦva$_s$	54.58	1.70	15.97	5.03	5.76	0.17	3.61	7.55	4.14	1.17	0.30	99.99
G17	17	basalt	Qvb$_{tch}$	50.21	1.11	17.91	4.90	5.61	0.17	7.07	8.77	3.73	0.32	0.19	99.99
G18	850716	quartz diorite	Riqd$_w$	67.22	0.49	17.05	1.89	2.16	0.08	1.48	4.94	3.61	0.92	0.16	100.00
G19	8597	basalt	Mvb	52.68	2.13	17.03	2.00	9.16	0.18	4.27	8.90	2.50	0.85	0.31	100.01
G20	8554	basalt	Mvb	52.77	2.00	16.78	5.33	6.11	0.17	4.29	8.53	2.73	0.95	0.33	99.99
G21	5539	basaltic andesite	MΦi	55.09	2.41	14.96	5.44	6.23	0.18	3.83	7.74	2.53	1.21	0.39	100.01
G22	5535	basaltic andesite	MΦi	55.26	1.43	17.97	4.34	4.97	0.16	3.86	6.52	4.12	1.14	0.23	100.00
G23	5534	andesite	MΦi	58.16	2.02	15.69	4.62	5.29	0.16	2.99	6.20	3.10	1.32	0.45	100.00

[1] Unit symbols conform to units from this study and do not always correspond to previous mapping.

MΦid **Diorite**—Dark gray to light brownish-gray, variably weathered, locally altered, fine- to medium-grained aphyric to felty diorite containing equigranular subhedral to anhedral, concentrically zoned plagioclase with intergranular texture, anhedral to recrystallized quartz, clinopyroxene, amphibole, sulfide minerals, and abundant clay minerals. Nearly all thin-section samples of diorite contain a pervasive, regular, and closely spaced shear fabric wherein plagioclase laths are rotated along shear planes, although plagioclase laths outside these zones are randomly oriented. Texture typically becomes cryptocrystalline adjacent to contacts with surrounding rock. Alteration is significant within a small diorite body on Sinter ridge, north of Trout Creek Hill (Plate). Diorite locally includes unmapped areas of gabbro and gabbroic diorite, especially within the intrusives underlying Buck Mountain. The mass at Buck Mountain also appears to be less weathered and/or altered, with locally glomeroporphyritic texture. Some exposures of the diorite appear to have cooled at shallow depth, exhibiting columnar jointing. Berri and Korosec (1983) obtained a K-Ar age of 23.2 ±1.0 Ma for the diorite from the southwest flank of Warren Ridge along the Wind River Highway (Plate, map no. 5; Table 2). Geochemistry for diorites sampled in this study (Plate, map nos. G1, G5, G6, G8, G9, G10, G14, and G15; Table 1) was originally published in Berri and Korosec (1983) and Korosec (1987). Subdivided into:

MΦidp **Diorite porphyry**—Highly weathered, light reddish-brown, pilotaxitic diorite with a fine-grained microlitic matrix with abundant clay mineralization and abundant plagioclase porphyry with secondary quartz intergrowth. This unit was noted only on the crest of Big Butte.

MΦigb **Gabbro**—Dark brownish-gray, equigranular to porphyritic, medium-grained gabbro composed of embayed plagioclase and pyroxene porphyry with minor alteration to hornblende; groundmass composed of plagioclase, clay minerals, and sulfide minerals. This gabbro is found predominantly on Bunker Hill, although this lithology was also noted locally within the large body of diorite on top of Warren Ridge, as well as in several dikes on the east and southeast flanks of Warren Ridge. We suspect the gabbro found within the diorite on Warren Ridge may also be dikes intruding the diorite. In addition, we mapped a small, poorly exposed, yet distinct body of hornblende gabbro porphyry near the top of Sinter ridge, north of Trout Creek Hill. Here, hornblende phenocrysts are large (2–3 mm), subrounded, and accompanied by smaller plagioclase phenocrysts in a fine-grained matrix containing plagioclase and minor quartz and orthopyroxene. The geochemistry for a sample of gabbro on Bunker Hill (Plate, map no. G3; Table 1) was originally published in Berri and Korosec (1983).

Table 2. Whole-rock K-Ar age determinations for the Wind River valley area. *, not shown on Plate.

Map no.	Geologic unit	Age (Ma)	Description	Source	Latitude	Longitude
1	Qvb$_{tch}$	0.34 ±0.07	Whole rock analysis performed at Oregon State University	Korosec (1987)	45.75597	-121.83693
2	Qvb$_{tch}$	0.34 ±0.07	Whole rock analysis performed at Oregon State University	Korosec (1987)	45.71777	-121.79962
3	Mvb	20.8 ±1.2	Whole rock analysis; average of two analyses	Korosec (1987)	45.86944	-121.92869
4	MΦi	22.7 ±0.9	Dike; whole rock analysis of dacite performed at Oregon State University; originally mapped as dacite flow within Ohanapecosh Formation	Berri and Korosec (1983); Korosec (1987)	45.79561	-121.93793
5	MΦid	23.2 ±1.0	Whole rock analysis performed at Utah Research Institute	Berri and Korosec (1983)	45.82262	-121.91332
6*	ΦEvc$_o$	32.8 ±0.8	Whole rock analysis performed at Mobil Research Laboratory; unit MΦvt(3) from Phillips (1987)	Phillips (1987)	45.75512	-122.05249
7*	MΦva	23.6 ±1.2	Whole rock analysis of andesite flow of Three Corner Rock; average of two analyses	Phillips (1987)	45.79284	-121.99975
8	Riq$_w$	4.9 ±0.8	Whole rock analysis on Wind Mountain diorite porphyry	Korosec (1987)	45.71247	-121.76224
9	Riq$_w$	6.6 ±0.7	Whole rock analysis on Wind Mountain diorite porphyry	Korosec (1987)	45.70349	-121.74607
10	MΦva$_s$	15.7 ±1.5	Whole rock analysis on Stevenson Ridge basaltic andesite	Korosec (1987)	45.74025	-121.84390

Eocene to Oligocene Volcaniclastic Rocks

ΦEvc$_o$ **Ohanapecosh Formation**—Massive, 1- to 3-meter-thick layers of matrix-supported, coarse-grained crystal-lithic and vitric lapilli tuff breccia, interlayered with a roughly equal amount of thinly bedded tuffs, pebbly diamictites, highly incompetent silty sandstones and siltstones, and other, less abundant, thinly to thickly bedded aquagene volcaniclastic deposits and thin basaltic lava flows. Bedding within thinly bedded volcaniclastic units is generally defined by primary ash content, as well as the amount and degree of sorting of larger clasts within clayey, weathered matrices. Tuff breccias are locally vesicular, and bed margins are frequently baked. Deformed fiamme were noted preferentially oriented parallel to layering, suggesting hot, subaerial deposition. Wise (1961) noted an abundance of logs within the lower portions of many tuff breccias. We also noted abundant woody debris within a relatively thick silty sandstone layer in borehole WRV-1, as well as in a limited number of outcrops.

Much of this unit is highly weathered to clay. In addition, alteration of this unit is highly variable and localized; typically, the matrices (and to a lesser degree, clasts) of the unit have been silicified and (or) zeolitized, and this alteration generally increases adjacent to intrusive bodies. Silicified tuff breccias and volcaniclastics are typically resistant and outcrop well. We noted minor contact metamorphism to hornfels at intrusive contacts.

Stratigraphy within the Ohanapecosh Formation in the area did not lend itself to mapping subunits, as exposure was poor enough to prohibit following individual flows or layers for any mappable distance. Nor were general rock types within this unit sufficiently thick or laterally continuous enough to do so. We also opted to not differentiate the upper stratigraphy of this unit, previously distinguished by Korosec (1987) as unit Tvt(3). We noted no stratigraphic marker or change, either by lithology or degree of weathering, defining the contact between the lower Miocene and Eocene–Oligocene volcaniclastics reported by Korosec (1987).

The age of this unit is ultimately not clear, and the anomalously young age reported in Berri and Korosec (1983) and Korosec (1984) may be based in part on a radiometric age obtained from a possibly misassigned dacitic rock sample. Fiske and others (1963) assigned an Eocene age to the unit, based on fossil leaf evidence. Fossils from an upper portion of the unit near Nelson Creek, south of the map area near the Columbia River, yielded an Oligocene age. A whole rock K-Ar age of 32.8 ±0.8 Ma (Phillips, 1987; Table 2) was obtained from tuffs and tuff breccias in this unit about 7 miles southwest of the map area. The age of the unit here is constrained to the Oligocene by (1) an age of 23.2 ±1.0 Ma (Korosec, 1987; Plate, map no. 5; Table 2) on dioritic intrusions in the unit, and (2) an age of 23.6 ±1.2 Ma (Phillips, 1987; Table 2) on andesite flows of Three Corner Rock overlying the unit about 3 miles west of the map area.

The geochemistry for tuff samples (Plate, map nos. G7 and G11; Table 1) was originally published in Berri and Korosec (1983).

Quaternary? to Eocene Tectonic Zones

tz **Tectonic zone**—Variably clay- and sand-rich fault gouge and fault breccia with abundant fractures and slickensided surfaces in which relationships between geologic units are highly disrupted and cannot be shown accurately at map scale. Unit is dark gray to green, mottled and altered, and contains numerous seeps and springs. This unit was mapped in only one location along the Wind River, at the junction of two faults in diorite (unit ₥Φid) and volcaniclastics (unit ΦEvc$_o$). Age is unclear.

GEOPHYSICAL SURVEYS

Geophysical surveys within the study area were conducted to delineate key geologic features where existing subsurface data was sparse. Given the local geology and project goals, we chose to employ two geophysical methods: (1) ground-based magnetics and (2) electrical resistivity. Both methods are proven to be cost- and time-effective and have the ability to produce high-resolution results.

A ground-based magnetic survey measures the local total magnetic field, which can change due to the amount of ferrous material present in the subsurface. This method allows for an extremely large amount of data to be collected over a short period of time and has effectively been used to identify key contacts and structural features.

An electrical resistivity survey is a subsurface imaging technique that generates an image of the electrical properties of the subsurface by passing an electrical current along electrodes and measuring the associated voltages. Characteristics that have the greatest effect on subsurface resistivity are the porosity and level of saturation of the subsurface material.

Ground-Based Magnetic Anomaly Survey

METHODOLOGY

The ground-based magnetic method uses a sensor to measure the local total magnetic field (that is, Earth's magnetic field plus the bedrock-induced magnetic field). It is assumed that the remanent magnetic field of local basalt flows would have little effect on the total magnetic field measured in relation to the contribution of Earth's magnetic field and the induced component. Therefore, any significant change in the measured total magnetic field is a direct result of a compositional change occurring in the subsurface. This method is particularly useful when trying to identify geologic features such as hydrothermally altered zones or faults that have juxtaposed differing rock types against each other.

We used a Scintrex ENVI-MAG proton-precession magnetometer with a resolution of 0.01 nT. This system has the ability to collect data in two different modes, stop-and-go and WALKMAG. We used the WALKMAG mode during this survey to take measurements along a survey line every two seconds. To reduce any magnetic interference during the survey, we used one operator (with all magnetic material removed) per survey line and removed or walked around all visible magnetic objects along the survey line. In the field, the position of the magnetometer was determined using GPS. The locations of survey lines were based on relationships made from field observations, as well as access to roads and trails with minimal cultural noise.

Collected magnetic data were downloaded from the magnetometer and attached to corresponding GPS data, based on synchronized time stamps. Each survey line was then filtered to remove measurements with a recorded noise value greater than 1.0 or that coincided with culture noise (that is, culverts, metal signs, bridges, etc.) noted during the survey. Most profiles underwent a manual filter as well to identify and remove obvious outliers. For this study, we were not interested in the total magnetic field being measured, but rather the relative change in amplitude of the total magnetic field; therefore, the total magnetic field amplitude for the remaining measurements was calculated by subtracting each measurement from the mean average of the associated survey line. There appeared to be a significant amount of high-frequency noise introduced during most of the surveys as a result of sensor jostling during the WALKMAG mode. To filter out the high-frequency noise, a weighted running average consisting of two measurements before and after each reading was calculated for each survey line.

RESULTS

In addition to refining the locations of mapped contacts, we identified several anomalous areas within numerous survey lines that indicate or confirm the presence of faults. For example, there is an abrupt change in the total field magnetic amplitude as profile 15 begins to reach the valley bottom at the northwest end. This abrupt change coincides with field observations that confirm the presence of the Brush Creek fault (*see* Alteration and Structure, p. 13). Additionally, along the northern extent of survey lines 16 and 17, we identified a large anomalous zone that continues for 135 meters, indicating a highly pervasive fracture pattern in the bedrock. This finding supports numerous field observations of faults in this area (*see* Fig. 5, p. 14).

Electrical Resistivity Survey

METHODOLOGY

The electrical resistivity method is an active-source geophysical technique that is capable of generating tomographic images of subsurface resistivity by noninvasively transmitting a direct-current signal into the ground and measuring the resulting voltages (potentials) at various positions. Electrical resistivity measurements are sensitive primarily to the porosity of subsurface material and the salinity of the fluid within saturated zones. This technique has been widely used in identifying depth to bedrock, water-bearing fault zones, and other saturated layers. Resistivity values of igneous rocks are typically high, ranging from 1,000 to 10 million Ω·m, depending on the degree of fracturing and the number of fractures filled with groundwater. Unconsolidated sediments generally have extremely low resistivity values ranging from 10 to 1,000 Ω·m (Loke, 2001).

We identified four areas within the study area that were: (1) large enough to accommodate the length of the profile, (2) contained minimal cultural noise, and (3) were considered of geologic interest. We used an automated 72-channel Syscal R1 Plus unit, which is capable of generating cross-sectional views of ground resistivity extending to depths of more than 100 meters under ideal conditions. Profiles ranged from 240 to 360 meters in length and used two types of arrays (dipole-dipole and Wenner-Schlumberger) with electrode spacings between 5 and 10 meters to maximize survey depth without compromising resolution. The transmitting injection time was set to 500 milliseconds. The minimum stacking ratio for each quadrature was three, provided the consistency between measurements was less than two percent; otherwise, the system collected up to a total of six measurements.

Resistivity data were processed and inverted using the *Res2DInv* software. Results for each profile are presented as colored 2-D electrical images of the subsurface (that is, a vertical cross section of the distribution of subsurface resistivity) in Appendix B. Profile images indicate a range of resistivity values from less than 100 to more than 5,000 Ω·m for the subsurface geology. Measured values with standard deviations larger than 2σ were removed and a topographic correction was applied to the entire profile before the data were processed using a damped least-squared procedure.

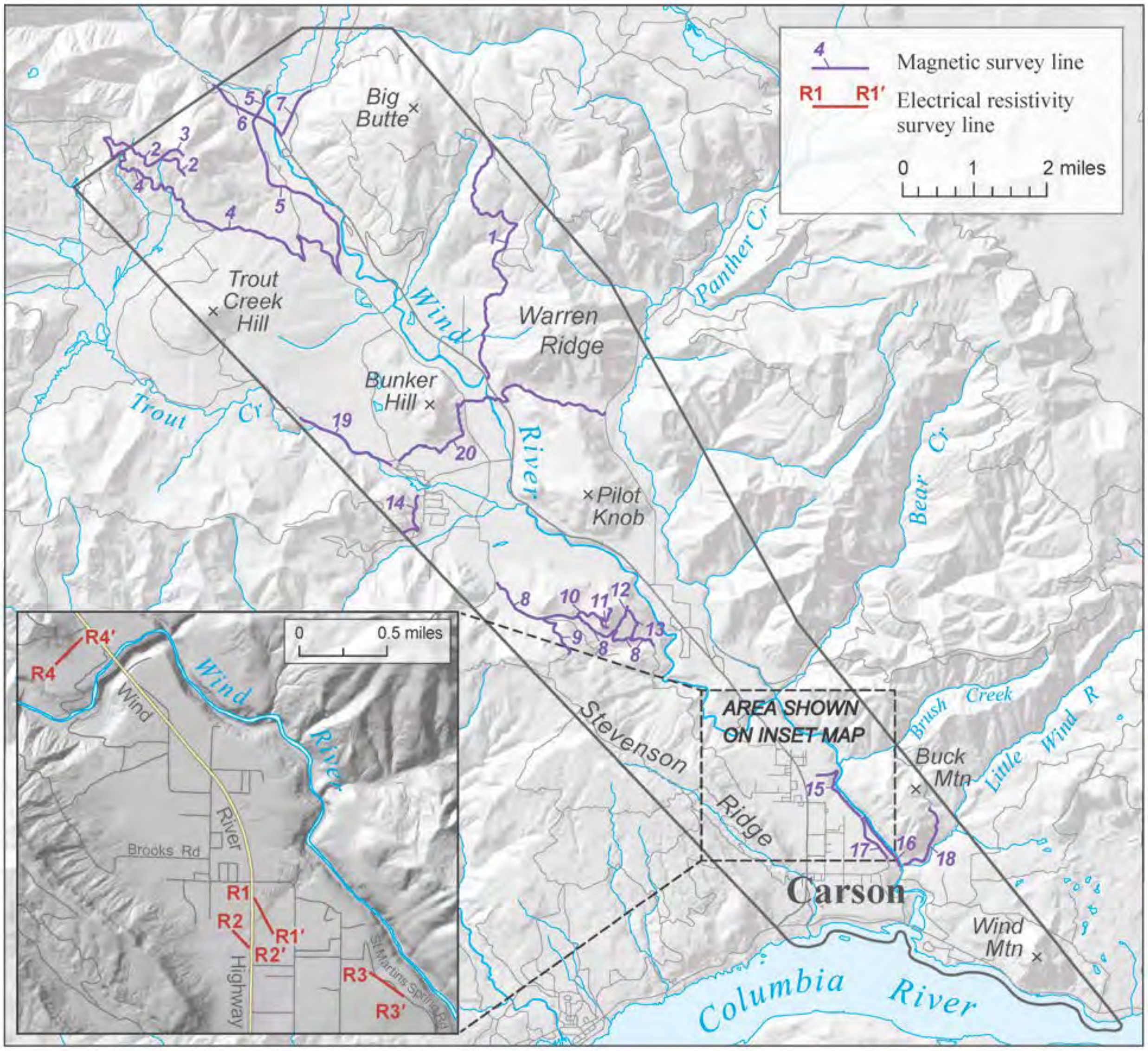

Figure 3. Shaded relief map of the Wind River valley and vicinity showing magnetometer and electrical resistivity survey transects.

RESULTS

Profiles R1 and R2 are located on WKO Inc. (High Cascade) property and were selected to provide further subsurface information on a NE–SW-trending linear topographic expression identified from lidar (Fig. 3) that appears to be an along-strike extension of faults mapped within the uplands to the northeast and southwest (*see* Alteration and Structure, p. 13). R1 has a total length of 240 meters with a maximum depth of 35 meters (Fig. B1). There is a sharp change in resistivity (150 to more than 1,200 Ω·m) at 20 to 25 meter depth that separates two lateral zones of low and high resistivity values. We interpret this sharp change in resistivity as the contact between highly fractured basalt (unit Qvb_{tch}) and overlying alluvium (unit Qs). This contact appears to be disturbed between 110 and 160 meters, and we infer that the resistivity change in the material beneath this zone coincides with either one strand or multiple strands of the Brush Creek fault.

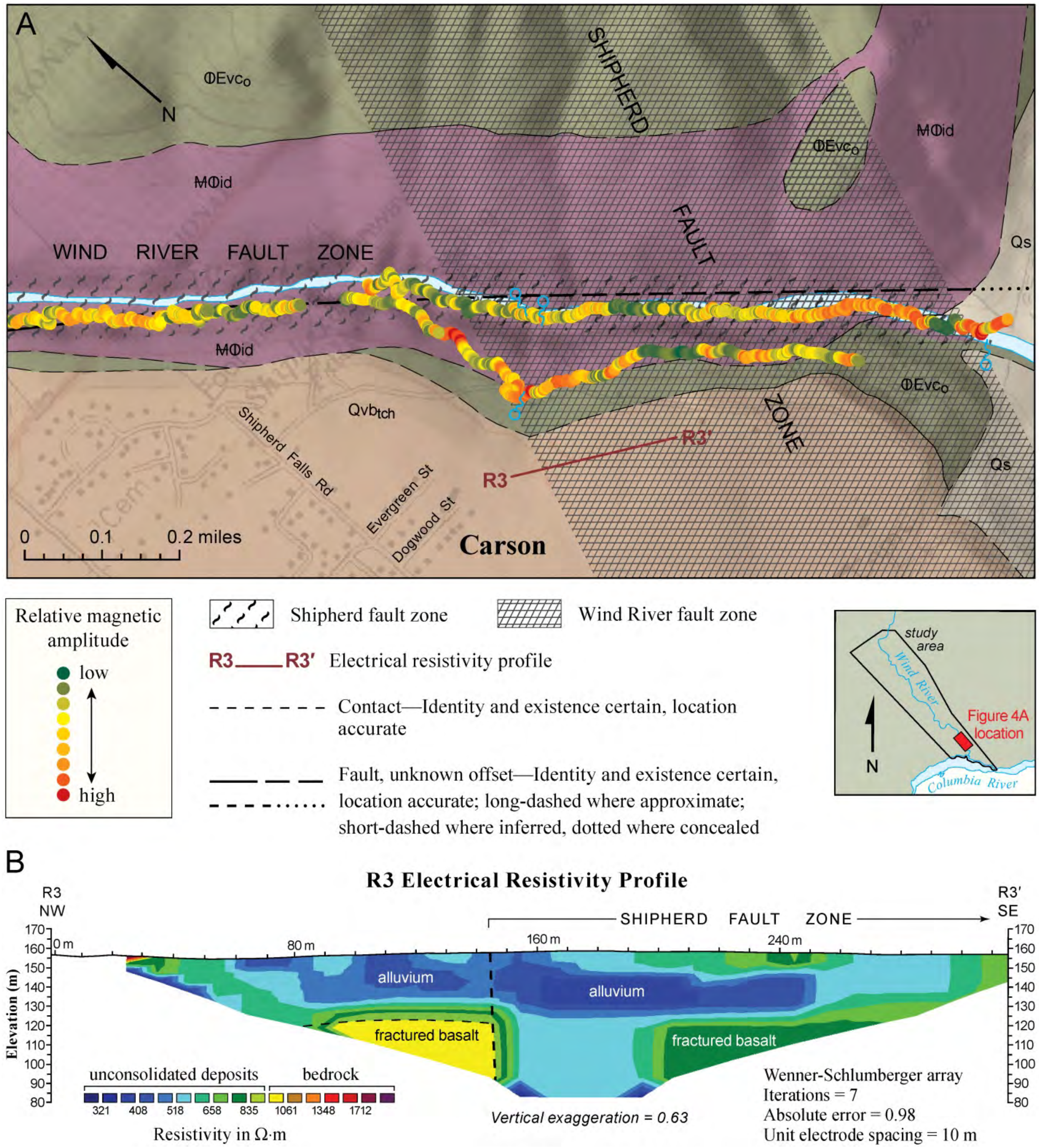

Figure 4. Shaded relief map of the lower Wind River valley showing correspondence between magnetic anomaly data, surficial geology, and electrical resistivity profile R3–R3′. Alluvium shown in resistivity profile not mapped at this location on Plate.

R2 has a total length of 270 meters and a maximum depth of 55 meters (Appendix B, Fig. B1). There is a similar sharp change in resistivity (150 to more than 1,200 Ω·m; see dashed black line on section R2–R2′ in Appendix B, Fig. B1) to that of R1, starting at less than 5 meters depth at the northwest end and increasing to about 20 meters depth at the southeast end. We infer that this sharp change in resistivity values represents the contact between Trout Creek Hill basalt (unit Qvb_{tch}) and overlying alluvium (unit Qs). There are two abrupt changes in depth along this contact: at 50 meters and 92 meters from the northwest end of the profile. The larger of these two anomalies coincides with the mapped Brush Creek fault.

Profile R3 was run on Carson Hot Springs Golf & Spa Resort property, trending roughly southeast, parallel to the Wind River (Fig. 3). This profile location was selected in an attempt to intersect an extension of the dense network of northeast-trending faults observed in the Wind River channel to the northeast. R3 has a total length of 360 meters with a maximum depth of 80 meters (Fig. 4; Appendix B, Fig. B2). There is a thick zone of low resistivity values across the upper portion of the profile that we interpreted as alluvium (unit Qs, not mapped), starting at the surface and extending to about 35 meters depth. We infer that Trout Creek Hill basalt lies beneath this layer and comprises the higher resistivity material. There is a smaller low-resistivity zone (~40 meters wide) in the center of the profile that extends to more than 80 meters depth and separates two more-resistant (800–1,000 Ω·m) zones on either side. We interpreted this as a shear zone near the northwest boundary of the Shipherd fault zone (Fig. 4).

Profile R4 trends northeast and is located immediately west of High Bridge on the northwest side of the Wind River (Fig. 3). The profile location was selected based on field observations of a highly deformed section of the Ohanapecosh Formation (unit ΦEvc$_{o}$) immediately north of the profile (Plate). R4 has a total length of 360 meters with a maximum depth of 60 meters (Appendix B, Fig. B2). There is an abrupt change in resistivity near the center of the profile that extends from less than 5 meters below the surface to the bottom of the profile. This abrupt change is part of a larger anomalous zone approximately 100 meters wide that likely represents a portion of the Wind River fault zone.

ALTERATION AND STRUCTURE

Primary layering of tuff breccia and volcaniclastic rocks of the Ohanapecosh Formation dips gently west-southwest, with a mean azimuthal strike and dip of 142/16 (Fig. 5A). Exceptions to this orientation occur near faults, or at or near contacts with dioritic intrusions, where layers are either deflected and upwarped by the intruding mass or deformed into series of poorly developed faults and folds. Deflection of this layering can easily be observed along the Wind River Highway between mile markers seven and eight, where a thinly to thickly interbedded sequence of volcaniclastics is upwarped into an apparent anticline surrounding a well-exposed underlying mass of diorite.

The gentle, southwest regional dip of bedding is likely responsible for the large slope failures of the west flank of Big Butte, as well as the large landslide south and southeast of Buck Mountain, where bedding dips are slope-parallel.

Several northeast-striking faults, likely associated with the western end of the Yakima fold and thrust belt, traverse the valley and uplands on either side of the Wind River at several locations: Bear Creek fault, Brush Creek fault, Shipherd fault zone, and a series of unnamed faults in the northern half of the map area (Plate).

An excellent exposure of Brush Creek fault is on a south-facing hillside on the north bank of the Wind River, approximately 1,500 feet southwest of the outlet of Brush Creek. It consists of more than 20 feet of highly sheared fault gouge (unit tz) and abundant mineral seeps (Fig. 5B; Plate). Farther to the southwest along trend, splays of this fault generate southeast-facing scarps within the broad valley floor. Offset of the Quaternary Trout Creek basalt flow (unit Qvb$_{tch}$) here is suggested by abrupt discontinuities in electrical resistivity profiles R1–R1′ and R2–R2′ (Appendix B, Fig. B1).

We also noted intense deformation and hydrothermal activity along a wide zone containing dense (5-meter spacing), subparallel, steeply southeast-dipping faults that bound and include the Shipherd's and St. Martins Hot Springs along the Wind River. We are calling this northeast-trending zone, the Shipherd fault zone (Fig. 5B; Plate). The northern boundary of this zone is marked by a dense network of faults just north of Shipherd's Hot Springs and multiple coincident magnetic anomalies in transects 16 and 17 (Fig. 3). A sharp anomaly within electrical resistivity profile R3–R3′ (Fig. 4) suggests that this zone offsets unit Qvb$_{tch}$ and underlying units west of the river canyon, although there is no topographic suggestion of this feature within the broad valley floor. At the southern end of the fault zone, exposed in the Wind River canyon, we noted a major fault strand visibly issuing gas bubbles as it traversed the river directly along trend with the St. Martins Hot Springs pump house. Many of the faults within this zone contain abundant gouge as much as 2 meters thick and (or) mineralization. There are numerous gas seeps evident along submerged faults throughout this zone. These faults consistently offset northwest-trending faults of the Wind River fault zone, and the intersections of these two sets of faults appear to control the locations of hot springs in the southern part of the valley. This finding is slightly different from that of Berri and Korosec (1983), who attributed spring activity at St. Martins Hot Springs to the Little Wind River fault, which they mapped along the Little Wind River on the southeast side of Buck Mountain. While we encountered abundant outcrops of

Ohanapecosh Formation along the Little Wind River, we found no structural evidence to support the existence of this fault.

Numerous oblate areas of intense alteration and silicification were noted on Sinter ridge, an east–west-trending ridge immediately north of Trout Creek Hill volcano (Plate). These areas are concentrated along several northwest–southeast-striking faults that cross the ridge. Abundant granulitic, highly vesicular, and locally amygdaloidal silica and aluminum-rich sinter with a locally penetrative crenulation cleavage (4-mm scale) lie within these zones and lines fractures in adjacent diorite bodies. A thin section of the sinter appears to show secondary quartz mineralization along small microfaults oblique to the crenulation cleavage. The diorite contains abundant blebs of recrystallized quartz. The alteration was likely produced by repeated movement of gas- and silica-rich fluid along faults and fractures within a geothermal system shortly after emplacement and cooling of the diorite. Timing of the alteration is unclear and could possibly be coeval with Quaternary Trout Creek Hill basalt emplacement.

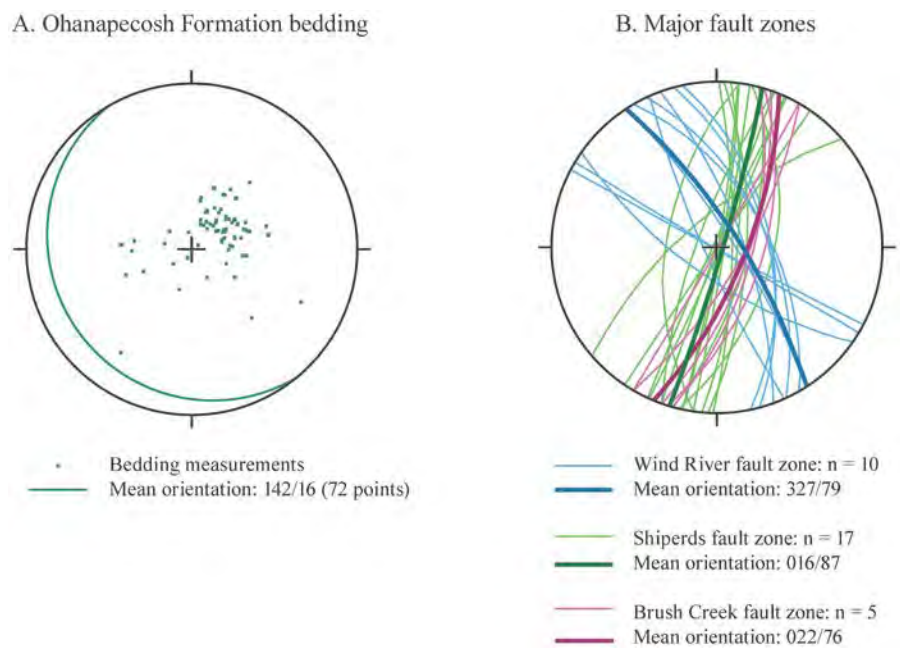

Figure 5. Equal-area stereonets showing structural data from the Wind River valley. **A.** Primary layering and bedding in the Ohanapecosh Formation shown as poles to planes. **B.** Major fault zones within the Wind River valley, shown as planes.

TEMPERATURE-GRADIENT DATA

In the early 1980s, DGER drilled three temperature-gradient boreholes, DNR-85-7C, DNR-7 (DNR-TRCK), and DNR-8 (DNR-CRSN), the first two located near the Stabler-Hemlock Ranger Station and the third near St. Martins Hot Springs (Fig. 1). The two boreholes near the Stabler-Hemlock Ranger Station yielded gradients between 75° and 79°C/km. Borehole DNR-8 yielded a recalculated gradient of 166°C/km, although earlier reports used a much higher gradient for this well. Elevated temperature gradients were previously measured in several pre-existing water wells, especially toward the southern end of the Wind River valley.

During August of 2012, a 287-foot-deep geothermal test hole (WRV-1) was drilled using air rotary methods on U.S. Forest Service land in the northern Wind River valley at an informal group campsite approximately 1,000 feet northwest of Tyee Springs (Plate). Factors used to locate the WRV-1 test hole included: (1) land and road access—U.S. Forest Service lands at a previously disturbed site along Wind River Highway, (2) a data gap for regional gradient modeling—while numerous wells were logged to the south, no well gradient information existed for this area of the valley, and (3) favorable pre-existing reconnaissance-scale data, including aeromagnetic anomaly, gravity, earthquake, water-well temperature, gradient/heat flow, and fault data, which suggested that high heat flow in the southern part of the valley may extend northward along a structural discontinuity.

Rock cuttings collected during drilling revealed approximately 45 feet of basalt of Indian Heaven (unit Qvb_{ih}) overlying a significant thickness of older Wind River alluvium containing substantial amounts of water. The older alluvium was prone to caving, and as a result, we opted to advance casing through this unit. Bedrock was encountered at a depth of 187 feet, consisting of a thick, poorly cemented, interbedded silty sandstone and siltstone section of the Ohanapecosh Formation. We reached a depth of 341 feet, but due to the tendency of the formation to cave and the abundance of water, the borehole backfilled from lower, uncased portions of the hole to 287 feet. Because of the extreme difficulty in maintaining an open hole, we ultimately opted to stop drilling and set the 2-inch casing to 287 feet, after conducting a downhole geophysical survey.

After a period of equilibration, we logged the cased borehole with temperature-gradient logging equipment on several occasions, yielding a final gradient of 55.9˚C/km. Following temperature-gradient logging, the borehole was plugged and abandoned in June of 2013. Appendix A (Figs. A1–A3) shows the boring log, well completion diagram (including temperature-depth plot), and geophysical log for this borehole.

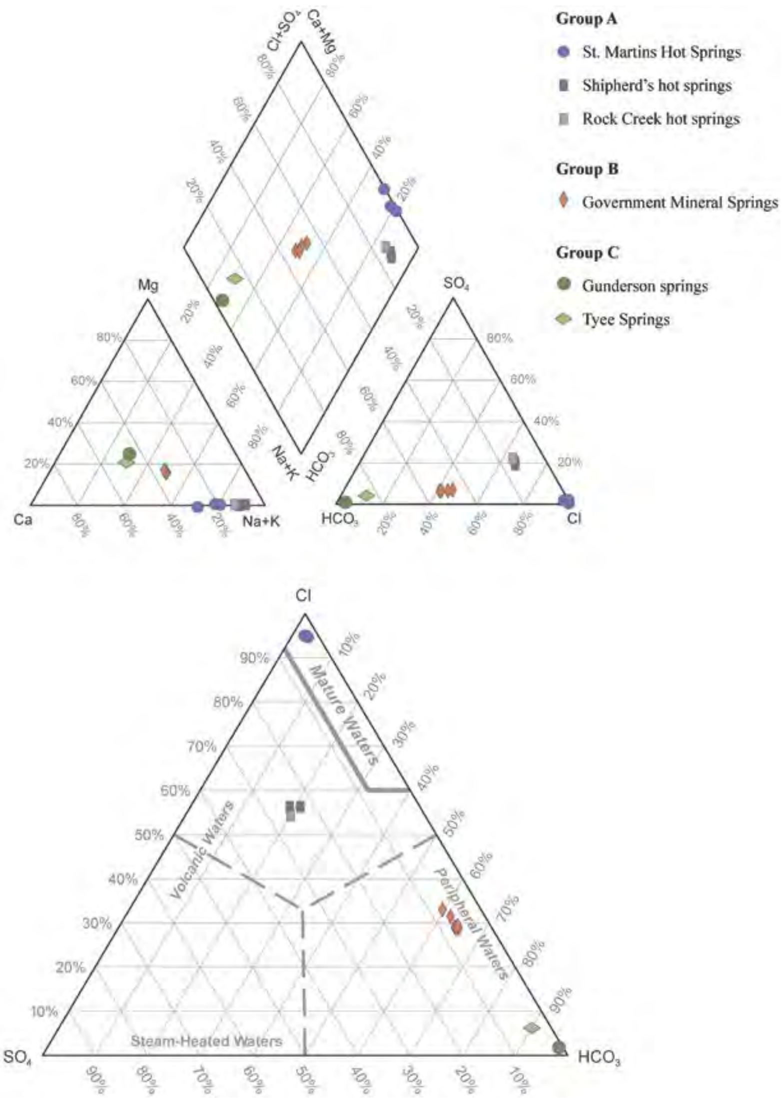

Figure 6. Piper diagram and Cl-SO_4-HCO_3 ternary diagram of six thermal and mineral springs in the Wind River valley and vicinity.

THERMAL AND MINERAL SPRINGS

There are numerous thermal and mineral springs in the Wind River valley, some of which are well known. It is likely that most of these springs are located along faults or intersection of faults either within or traversing the valley. Based on spring chemistry and geologic setting, these springs can be placed into three groups.

Group A springs are fault-related. Bedrock along and within the entire length of the Wind River valley southwest of Buck Mountain is densely faulted, and numerous springs are found where the two major sets of fault orientations previously discussed in 'Alteration and Structure' intersect (Plate). Shipherd's and St. Martins Hot Springs are of this type (Fig. 1). Both Shipherd's and St. Martins Hot Springs are set in faults within diorite bedrock and are associated with gas bubbling from numerous dispersed fault planes. High temperatures of 40.8° and 50˚C were recorded for these springs. Rock Creek Hot Springs is located within Rock Creek, along trend with a northwest-trending fault mapped by Hammond (1980)(Fig. 1). A temperature of 33.5˚C was reported for this spring (Korosec, 1983). Collins Hot Springs is now buried by the Columbia River (Korosec, 1980), but its location is along strike with a northeast-trending fault mapped by Hammond (1980)(Fig. 1).

Spring chemistry data gathered from literature and our recent sampling program indicate that Group A springs are strongly Na-Cl dominant, partially equilibrated, and based on their Cl-SO_4-HCO_3 content, can be classified as mature (St. Martins Hot Springs) to mixed (Shipherd's Hot Springs) waters (Fig. 6, Table 3)(Marini, 2000). Geothermometer calculations for high-quality chemical analyses yield average estimated source-reservoir temperatures of 65˚C (Na-K-Ca) and 73˚C (chalcedony conductive) for St. Martins Hot Springs (Powell and

Cummings, 2012). Similar calculations for Shipherd's Hot Springs yield an estimated Na-K-Ca source temperature of 19˚C. No chemical data for Collins Hot Springs could be found in published literature, although a surface temperature of 40° to 50˚C was estimated for this water (Korosec, 1980) Group B springs consist of Government Mineral Springs and Little Soda Springs; both are, or were, located at the northern end of the study area. Government Mineral Springs consists of numerous weakly bubbling orange-tinted cold springs set in deep alluvium along and within Trapper Creek (Fig. 1), as well as a manual-pump well developed within the same system (Iron Mike Well). Their chemistry indicates no dominant cation or anion (Fig. 6, Table 3) and can be classified as Na-HCO_3 peripheral waters (Marini, 2000); geothermometer calculations for high-quality chemical analyses yield average estimated source-reservoir temperatures of 59˚C (Na-K-Ca) and 66˚C (alpha cristobalite)(Powell and Cummings, 2012). Little Soda Springs is located approximately 1.5 miles to the southeast of Government Mineral Springs within boggy lowlands adjacent to the Wind River (Fig. 1). Recent attempts to locate this spring failed, and previously published chemistry from this spring had an extremely high charge balance, so was not included here.

Group C springs consist of Gunderson Springs and Tyee Springs. Gunderson Springs is a series of small cold seeps along the same structural zone as Shipherd's and St. Martins Hot Springs, but the springs issue out of overlying landslide deposits along the Wind River at its junction with the Little Wind River, south of the southern boundary of the Shipherd fault zone (Fig. 1). Water chemistry indicates that the spring is a Ca-HCO_3 dominant peripheral spring, and we suspect that the sample is highly dilute due to its disconnect from bedrock as well as the high-flow conditions at the time of sampling. Tyee Springs, a high-flow cold spring in the northern part of the map area, has chemistry similar to that of Gunderson Springs (Fig. 6; Table 3). Based on the heavy groundwater flow we encountered in the nearby WRV-1 borehole at shallow depth, it is likely that the water issuing from Tyee Springs is essentially a surface expression of fast-moving groundwater (through lava tubes?) in basalt of Indian Heaven.

DISCUSSION

Geologic mapping of the Wind River valley revealed the presence of a network of Miocene-age dikes that had previously been interpreted as either interbeds within the Ohanapecosh Formation or part of larger intrusive bodies. These dikes roughly parallel the trend of the valley, suggesting that a northwest–southeast-oriented zone of weakness has existed since Miocene time.

Pervasive fossil hydrothermal alteration along faults and some dikes in the northern part of the study area suggests that this area was a likely a geothermally active resource at one time. Measured temperature-gradients in wells in the northern part of the valley are slightly higher than background values, yet are not overly encouraging, and when considered along with spring chemistry from immature and dilute waters, suggest that additional exploration is not warranted.

Detailed mapping and geophysical surveys have provided evidence for several newly mapped faults, two of which likely offset a middle Pleistocene lava flow. Hydrothermal activity exists at the intersections of strands of the Brush Creek fault and the Shipherd and Wind River fault zones in the southern part of the valley along and within the Wind River canyon to the west of Buck Mountain. Elevated well temperatures and high gradients from nearby wells support this finding. While temperature gradients in this area are elevated, including an isolated gradient of 166˚C/km measured near this zone, spring water chemistry suggests that source temperatures at depth are insufficient for power generation. Exploitation of any low-temperature geothermal resources in this area should likely be directed to areas within hanging walls of these fault zones at or near fault intersections.

Northeast-trending faults in the lower part of the Wind River valley appear to be relatively young and likely form barriers to downvalley groundwater flow. Unlike areas to the north where shallow groundwater is abundant, very few wells have been drilled in the town of Carson (Plate) due to the apparent unavailability of shallow groundwater, and so surface waters are heavily relied upon for domestic use. Because of projected demand-increases and depletion of existing surface waters, additional sources of groundwater are currently being sought by the Skamania County Public Utility District. Any development of geothermal resources in the lower part of the valley would require the localized lack of shallow water in the southern part of the valley floor be taken into consideration; it is possible that any shallow groundwater encountered in new wells may be piped along fault zones rather than sourced from a regional or valley flow regime.

While several temperature-gradient boreholes exist at the mouth of the Wind River valley, one or more additional deeper (>2,000 feet) boreholes at or near fault intersections would likely provide valuable heat-flow information.

Table 3. Major element chemistry and isotope data for thermal and mineral springs in the Wind River valley and vicinity. Numbers in the Source column correspond to data sources listed at the end of the table. – –, no data; BDL, below detection limit of laboratory analysis.

GROUP A SPRINGS

Site	Sample ID	Date	Source	Units	Temp. °C	pH	Conductivity (µmhos)	SiO_2	Ca	Mg	Na	K	Fe	Li	HCO_3	SO_4	Cl	F	B	H_2S	CO_3	TDS	NH_4	As	Rb	Br	Cs	Sr	Mn	Charge balance (%)	Δ ^{18}O (%)	Δ D (%)	3He/4He ratio
Shipherd's Hot Springs	Shiperds H.S.	9/25/2012	1	none	– –	– –	– –	– –	– –	– –	– –	– –	– –	– –	– –	– –	– –	– –	– –	– –	– –	– –	– –	– –	– –	– –	– –	– –	– –	– –	– –	– –	2.90
	SPA-1	3/17/1981	3	ppm	40.8	8.5	220	47	4.2	0.1	43	BDL	BDL	BDL	– –	12	38	0.4	30	– –	– –	– –	– –	– –	– –	0.6	– –	– –	– –	22	– –	– –	– –
	– –	– –	4	ppm	42	8.5	220	47	4.2	0.1	43	BDL	BDL	BDL	– –	12	38	0.4	– –	– –	– –	135	– –	– –	– –	0.6	– –	– –	– –	22	– –	– –	– –
	Shiperds-12	8/27/2012	1	mg/L	40.0	9.67	250	42	3.8	<0.5	42	0.6	<0.05	<0.1	4	12	32	0.5	1.0	<0.001	– –	160	– –	0.009	<0.002	<0.2	<0.002	– –	0.003	26	-11.82	-86.3	– –
	Shiperds-2-13	6/12/2013	1	mg/L	31.8	9.32	247	22	3.7	<0.2	46	0.36	0.047	0.0075	11	12	30	0.35	1.1	0.138	36	160	0.12	0.011	– –	<0.2	<0.0001	– –	0.0016	6	– –	– –	– –
	SHS-3-13	6/12/2013	1	mg/L	25.5	9.32	231	21	4.4	<0.2	45	<0.2	0.031	0.0075	8.5	11	25	0.31	0.97	0.141	42	150	0.064	0.011	– –	<0.2	<0.0001	– –	0.00086	6	– –	– –	– –
St. Martins Hot Springs	St. Martins H.S.	9/25/2012	1	none	– –	– –	– –	– –	– –	– –	– –	– –	– –	– –	– –	– –	– –	– –	– –	– –	– –	– –	– –	– –	– –	– –	– –	– –	– –	– –	– –	– –	2.83
	29	– –	2	ppm	49	7.0	– –	BDL	104	BDL	291	6.2	0	0.2	– –	– –	636	– –	– –	– –	– –	– –	– –	– –	– –	– –	– –	0.1	BDL	0	– –	– –	– –
	CHS-12	8/8/2012	1	mg/L	45.3	7.79	2310	48	75	1.3	320	5.7	0.1	0.29	16	17	640	0.7	3.0	0.20	– –	1400	– –	0.003	0.012	6.1	0.002	– –	0.012	-2	-11.47	-95.1	– –
	SK008Sb	7/26/1977	5	ppm	48	8.54	2330	48	76	0.3	360	6.4	<0.02	0.28	19	16	690	0.74	2.9	<1	– –	1210	– –	– –	<0.02	– –	<0.1	– –	0.01	-1	– –	– –	– –
	SMA-1	– –	2	ppm	32	– –	2350	57	73	0.5	360	6	– –	0.30	– –	– –	756	– –	– –	– –	– –	– –	– –	– –	– –	– –	– –	– –	– –	-4	– –	– –	– –
	SMA-2	6/10/1981	6	ppm	50	8.5	2200	51	68	0.4	325	5.2	BDL	0.4	– –	16	680	0.6	22	– –	– –	– –	– –	– –	– –	7.3	– –	– –	– –	-5	– –	– –	– –
	– –	– –	4	ppm	53	8.5	2200	51	68	0.4	325	5.2	BDL	0.4	22	16	680	0.6	– –	– –	– –	1410	– –	– –	– –	7.3	– –	– –	– –	-6	– –	– –	– –
Rock Creek Hot Springs	RCA-1	8/25/1981	3	ppm	33.5	9.7	400	41	11.5	– –	80	0.1	– –	– –	31	40.0	85	0.7	– –	– –	– –	– –	– –	– –	– –	– –	– –	– –	– –	4	– –	– –	– –
	RCA-2	9/11/1981	3	ppm	33.4	9.3	400	– –	11.5	BDL	– –	0.1	BDL	BDL	– –	– –	85	0.7	– –	– –	– –	– –	– –	– –	– –	1.1	– –	– –	– –	-62	– –	– –	– –

GROUP B SPRINGS

Site	Sample ID	Date	Source	Units	T °C	pH	Cond. (µmhos)	SiO_2	Ca	Mg	Na	K	Fe	Li	HCO_3	SO_4	Cl	F	B	H_2S	TDS	NH_4	As	Rb	Br	Cs	Sr	Mn	Charge balance (%)	Δ ^{18}O (%)	Δ D (%)
Government Mineral Springs	– –	– –	7	mg/l	10	– –	– –	25-75	154	– –	176	5.1	– –	– –	– –	– –	276	– –	– –	– –	– –	– –	– –	– –	– –	– –	– –	– –	33	– –	– –
	– –	7/26/1977	8	mg/l	15	6.41	4680	75	360	100	585	14	0.06	1	1610	170	820	0.16	21	<1	– –	<1	– –	0.02	1.9	<0.1	– –	2.6	-1	-11.1	-79
	22	– –	9	ppm	8.5	6.5	– –	50	154	42.8	176	5.1	– –	0.3	– –	– –	276	– –	– –	– –	– –	– –	– –	– –	– –	– –	0.4	0.88	42	– –	– –
	GVA-1	3/17/1981	3	ppm	6.7	6	3900	68	268	91	420	9	15	0.9	– –	120	640	0.05	– –	– –	– –	– –	– –	– –	7	– –	– –	– –	32	– –	– –
	– –	– –	7	mg/l	8.5	– –	– –	20-60	192	– –	211	6.2	– –	– –	– –	– –	318	– –	– –	– –	– –	– –	– –	– –	– –	– –	– –	– –	36	– –	– –
	– –	– –	6	ppm	6.7	6	3900	68	268	91	420	9	15	0.9	– –	120	640	0.05	1000	– –	– –	– –	– –	– –	– –	– –	– –	– –	32	– –	– –
	– –	4/2/1980	10	mg/l	6	5.97	3650	64	260	75	420	9	14	– –	1230	120	550	0.12	15	<1	– –	1	– –	– –	1.2	– –	1.4	1.9	0	-11.12	-82.3
	– –	7/25/1980	10	mg/l	10	5.9	3534	66	270	76	440	9.2	– –	– –	1260	130	575	0.12	17	<1	– –	0.65	– –	– –	– –	– –	1.4	– –	-1	-11.09	-81.7
	– –	– –	6	mg/l	– –	– –	– –	– –	295	76	– –	– –	– –	– –	– –	– –	575		17	– –	– –	– –	– –	– –	– –	– –	– –	– –	13	– –	– –
	– –	7/26/1977	10	mg/l	18	6.01	3500	65	260	80	420	9.1	13	0.76	1250	120	570	0.12	15	<1	– –	<1	– –	<0.02	– –	<0.1	– –	2.4	0	– –	– –
	19	– –	9	ppm	10	7	– –	40	192	50.1	211	6.2	– –	0.4	– –	– –	318	– –	– –	– –	– –	– –	– –	– –	– –	– –	0.5	0.83	44	– –	– –
	GMS-12	8/8/2012	1	mg/l	11.0	6.19	2630	49	170	52	300	7.0	9.5	0.6	720	87	400	0.1	12	– –	1500	– –	<0.002	0.011	4.2	<0.002	– –	1.4	3	– –	– –
	24	– –	7	ppm	10	6.5	– –	BDL	309	82.4	404	9.6	– –	0.8	– –	– –	561	– –	– –	– –	– –	– –	– –	– –	– –	– –	0.6	2.11	43	– –	– –
Little Soda Spring	25	– –	6	ppm	8	6	– –	BDL	46	16.2	28	13.6	– –	BDL	0	0	36	– –	– –	– –	– –	– –	– –	– –	– –	– –	BDL	BDL	67	– –	– –
	LTA-1	3/17/1981	3	ppm	7.7	6	4000	47	218	200	310	3.5	1.6	BDL	– –	57	48	0.06	1350	– –	– –	– –	– –	– –	6.0	– –	– –	– –	88	– –	– –

Table 3. Major element chemistry and isotope data for thermal and mineral springs in the Wind River valley and vicinity *(continued)*

GROUP C SPRINGS																														
Site	Sample ID	Date	Source	Units	T °C	pH	Cond (µmhos)	SiO_2	Ca	Mg	Na	K	Fe	Li	HCO_3	SO_4	Cl	F	B	H_2S	CO_3	TDS	NH_4	As	Rb	Br	Cs	Sr	Mn	Charge balance (%)
Tyee Springs	TS-12	4/23/2012	1	mg/l	8	6.83	44	14	3.8	1.1	2.4	<0.5	0.05	<0.1	17	0.7	1.2	<0.1	<0.05	0.06	– –	31	<0.1	<0.002	<0.002	<0.2	<0.1	– –	<0.002	12
Gunderson Springs	Gunderson-13	6/12/2013	1	mg/L	11.4	6.10	142.8	17	11	3.7	7.8	0.57	2.2	<0.0001	58	<0.3	1.2	0.045	<0.01	– –	<5	80	0.039	0.00075	– –	<0.2	<0.0001	– –	0.29	5

1, Washington Division of Geology and Earth Resources, 2013, Field data collected during the 2010-2013 National Geothermal Data System project.
2, Korosec and others (1980)
3, Korosec, M. A. (1982)
4, Berri and Korosec (1983)
5, Korosec, M. A. (1984)
6, Korosec and others (1983)
7, Gizienski and others (1975)
8, Mariner and others (1982)
9, Campbell and others (1970)
10, Mariner and others (2006)

ACKNOWLEDGMENTS

Geologic mapping, geophysical surveys, spring sampling, and borehole drilling were funded by both the U.S. Forest Service under award no. AG-046W-P-11-0108 and by U.S. Department of Energy National Geothermal Data System grant no. DE-EE0002850. Wilkins Kaiser & Olson, Inc., Carson Hot Springs Golf & Spa Resort, D. Gunderson, and Ms. B. Acker graciously provided land access for geophysical surveys. Shawn Lombardini (DNR) assisted in the field. We would also like to thank Tom Vance (Skamania County Public Utility District) for water well reports and maps, and the Columbia Gorge Riverside Lodge, for their generous accommodations during field work.

REFERENCES CITED

Bela, J. L., compiler, 1982, Geologic and neotectonic evaluation of north-central Oregon—The Dalles 1 degree by 2 degree quadrangle: Oregon Department of Geology and Mineral Industries Geological Map Series GMS-27, 2 sheets, scale 1:250,000. [http://www.oregongeology.org/sub/publications/GMS/gms027_1.pdf (geologic map) and http://www.oregongeology.org/sub/publications/GMS/gms027_2.pdf (neotectonic maps)]

Berri, D. A.; Korosec, M. A., 1983, Geological and geothermal investigation of the lower Wind River valley, southwestern Washington Cascade Range: Washington Division of Geology and Earth Resources Open File Report 83-5, 48 p., 2 plates. [http://www.dnr.wa.gov/publications/ger_ofr83-5_wind_river_geology_24k.pdf]

Campbell, K. V.; Miers, J. H.; Nichols, B. M.; Oliphant, Jerrelyn; Pytlak, S. R.; Race, R. W.; Shaw, G. H.; Gresens, R. L., 1970, A survey of thermal springs in Washington State: Northwest Science, v. 44, no. 1, p. 1-11.

Fiske, R. S.; Hopson, C. A.; Waters, A. C., 1963, Geology of Mount Rainier National Park, Washington: U.S. Geological Survey Professional Paper 444, 93 p., 1 plate. [http://pubs.er.usgs.gov/usgspubs/pp/pp444]

Gizienski, S. F.; McEuen, R. B.; Birkhahn, P. C., 1975, Regional evaluation of the geothermal resource potential in central Washington State: Woodward-Gizienski and Associates, 113 p.

Hammond, P. E., 1980, Reconnaissance geologic map and cross sections of southern Washington Cascade Range, latitude 45 degrees 30 minutes – 47 degrees 15 minutes N., longitude 120 degrees 45 minutes – 122 degrees 22.5 minutes W.: Portland State University Department of Earth Sciences, 31 p., 2 plates.

Korosec, M. A., 1980, Thermal and mineral spring investigations, 1978–1979 (surveys and analyses). *In* Korosec, M. A.; Schuster, J. E.; and others, The 1979–1980 geothermal resource assessment program in Washington: Washington Division of Geology and Earth Resources Open File Report 81-3, p. 41-92. [http://www.dnr.wa.gov/publications/ger_ofr81-3_geothermal_resources_24k.pdf]

Korosec, M. A., 1982, Table of chemical analyses for thermal and mineral spring and well waters collected in 1980 and 1981: Washington Division of Geology and Earth Resources Open File Report 82-3, 5 p. [http://www.dnr.wa.gov/publications/ger_ofr82-3_spring_well_analyses.pdf]

Korosec, M. A., 1983, Surveys and geochemical analyses of thermal and mineral springs in Washington, 1980-1981. *In* Korosec, M. A.; Phillips, W. M.; Schuster, J. E.; and others, The 1980-1982 geothermal resource assessment program in Washington: Washington Division of Geology and Earth Resources Open File Report 83-7, p. 8-67. [http://www.dnr.wa.gov/publications/ger_ofr83-7_geothermal_survey.pdf]

Korosec, M. A., 1984, Chemical analyses for thermal and mineral springs examined in 1982–1983: Washington Division of Geology and Earth Resources Open File Report 84-1, 8 p. [http://www.dnr.wa.gov/publications/ger_ofr84-1_spring_ analyses.pdf]

Korosec, M. A., compiler, 1987, Geologic map of the Hood River quadrangle, Washington and Oregon: Washington Division of Geology and Earth Resources Open File Report 87-6, 40 p., 1 plate, scale 1:100,000. [http://www.dnr.wa.gov/Publications/ ger_ofr87-6_geol_map_hoodriver_100k.zip]

Korosec, M. A., 1989, New K-Ar age dates, geochemistry, and stratigraphic data for the Indian Heaven Quaternary volcanic field, south Cascade Range, Washington: Washington Division of Geology and Earth Resources Open File Report 89-3, 42 p. [http://www.dnr.wa.gov/publications/ger_ofr89-3_indian_heaven_age_date.pdf]

Korosec, M. A.; Phillips, W. M.; Schuster, J. E.; and others, 1983, The 1980–1982 geothermal resource assessment program in Washington: Washington Division of Geology and Earth Resources Open File Report 83-7, 299 p. [http://www.dnr.wa.gov/publications/ger_ofr83-7_geothermal_survey.pdf]

Korosec, M. A.; Schuster, J. E.; and others, 1980, The 1979–1980 geothermal resource assessment program in Washington: Washington Division of Geology and Earth Resources Open File Report 81-3, 270 p. [http://www.dnr.wa.gov/publications/ger_ofr81-3_geothermal_resources_24k.pdf]

Loke, M. H., 2001, Tutorial—2D and 3D electrical imaging surveys. *In* Course Notes for USGS Workshop '2D and 3D Inversion and Modeling of Surface and Borehole Resistivity Data', 13-16 March 2001, Storrs, CT.

Mariner, R. H.; Presser, T. S.; Evans, W. C., 1982, Chemical and isotopic composition of water from thermal and minerals springs of Washington: U.S. Geological Survey Open-File Report 82-98, 18 p. [http://pubs.er.usgs.gov/publication/ofr8298]

Mariner, R. H.; Venezky, D. Y.; Hurwitz, S., 2006, Chemical and isotopic database of water and gas from hydrothermal systems with an emphasis for the western United States: U.S. Geological Survey Digital Data Series 169. [http://hotspringchem.wr.usgs.gov/].

Marini, Luigi, 2000, Geochemical techniques for the exploration and exploitation of geothermal energy: Università degli Studi di Genova, Italia, 82 p.

Phillips, W. M., compiler, 1987, Geologic map of the Vancouver quadrangle, Washington: Washington Division of Geology and Earth Resources Open File Report 87-10, 27 p., 1 plate, scale 1:100,000. [http://www.dnr.wa.gov/Publications/ger_ofr87-10_geol_map_vancouver_100k.zip]

Powell, Tom; Cumming, William, 2012, Spreadsheets for geothermal water and gas geochemistry [3rd edition]: Proceedings, Thirty-fifth Workshop on Geothermal Reservoir Engineering, SGP-TR-188, [10 p.].

Wise, W. S., 1961, The geology and mineralogy of the Wind River area, Washington, and the stability relations of celadonite: Johns Hopkins University Doctor of Philosophy thesis, 2 v., 2 plates.

Wise, W. S., 1970, Cenozoic volcanism in the Cascade mountains of southern Washington: Washington Division of Mines and Geology Bulletin 60, 45 p., 1 plate. [http://www.dnr.wa.gov/publications/ger_b60_cenozoic_volcanism_cascades.pdf]

Appendix A. WRV-1 Well Data

Figure A1. Temperature-gradient well WRV-1 boring log.

Project: 2012 WADGER Geothermal Drilling Project location: Upper Wind River Valley Project number: 26L-RVS		Log of boring WRV-1 Sheet 1 of 5
	Logged by: J. Czajkowski / J. Bowman	Drill start date: 8/6/2012
	Checked by: J. Czajkowski	Drill end date: 8/27/2012
Total depth of borehole (ft): 286.5	Borehole diameter (in.): 10"/8"6"	Drilling method: air rotary
Approximate surface elevation (ft): 1151	Sampling method(s): grab	Drilling contractor: Schneider Equipment & Drilling Services
Groundwater depth (ft): 26	Legal location description: SE¼NE¼ sec.31 T05N R07E	

Depth (ft)	Sample I.D. (ft)	Time	Drill rate (ft/min)	Rock type	Material description	Remarks
0	1	2:35pm			0'—ALLUVIUM: moderate brown (5YR 3/4), loose, slightly moist to	0'—begin drilling and installation
					dry, poorly sorted, organic-rich, silty loamy soil with abundant silt; some	of 16" conductor casing, at 3.5'
		8/7/12 7:25am	0.24		broken glass and few rounded pebbles	excess silt required additional
	2	7:52am			6'—BASALT OF INDIAN HEAVEN: grayish black (N2), unweathered,	conductor casing and drilling foam
10					aphanitic to porphyritic, highly vesicular basalt with abundant zeolite-filled	
		8:52am			vugs, with sparse intermittent zones of lesser competence; possibly flow	11–12'—drilling fluid color
			0.61		top?	change, light gray to light brown
	3	9:01am				12'—softer material
20						22.5'—slower drilling
		9:28am	0.19		22.5'—competent vesicular basalt with abundant euhedral plagioclase	25'—slighly softer material
					laths	26'—static water level
	4 (29.5)	9:36am	0.45			
30		9:57am				34'-36'—water; drilling fluid
		10:15am	0.33		34–36'—abundant silt; interbed or void fill?	color change from light gray to
						light grayish tan
	5 (38)	10:23am	0.43			39–43'—slow drilling
40		10:38am			43'—abundant fragments of highly oxidized basalt; oxidized	43'—fast drilling; abundant water
		11:18am	0.18		zones moderate reddish brown (10R 4/6); loose; oxidation	45'—very fast drilling, abundant
					discrete & localized, fractured with rough fracture surfaces	water, >500 gal/min
		11:22am	1.13			49.5'—very fast drilling
50	6 (51.5)	12:55pm 12:56pm	2.5		51'—ALLUVIUM: sandy gravel, with abundant rounded pebbles of	51'—color change to light reddish
		8/9/12 12:36pm			various lithology; minor to trace clasts of altered tuff breccia;	brown fluid
					poorly sorted clasts with well-sorted very coarse, quartz-rich sand	53'—very fast drilling
	7 (58-63)		2			
60		12:41pm			63–64'—well-sorted pea gravel	63'—abundant caving; careful
		1:04pm				drilling
			3.4			
	8	1:27pm			66–99'—gravelly sand, pea-size gravel	
70						

Project: 2012 WADGER Geothermal Drilling Project location: Upper Wind River Valley Project number: 26L-RVS		Log of boring WRV-1 Sheet 2 of 5
	Logged by: J. Czajkowski / J. Bowman	Drill start date: 8/6/2012
	Checked by: J. Czajkowski	Drill end date: 8/27/2012
Total depth of borehole (ft): 286.5	Borehole diameter (in.): 10"/8"6"	Drilling method: air rotary/casing advance
Approximate surface elevation (ft): 1151	Sampling method(s): grab	Drilling contractor: Schneider Equipment & Drilling Services
Groundwater depth (ft): 26	Legal location description: SE¼NE¼ sec.31 T05N R07E	

Depth (ft)	Sample ID (ft)	Time	Drill rate (ft/min)	Rock type	Material description	Remarks
70		1:27pm	0.4			
		1:37pm				74'—grout bottom of hole to
		8/10/12 8:15am				reduce caving
	9 (78)					8/10/12—caved again to 62',
80		8/15/12 9:50am	0.4			thickened mud; caved to 62'
		9:55am				again after drilling to 83';
	10 (87)	10:55am 11:01am	0.33			abundant water
		11:08am	1.5			8/15/12—began casing advance
90						method
	11 (99)				99–109'—primarily sand with small amounts of pea-sized gravel	99'—casing advance deflector
100						around drill stem dislodged;
						sample taken from material
	(105)	11:20am				falling on deck
	12 (109)	1:07pm	0.18		109–135'—fine to coarse sand	109'—deflector dislodged again,
110						sample taken from deck; blooie
						line hose clogged with
						material
120						
	13 (125)	1:18pm				125'—deflector dislodged again;
		3:10pm	3.4			sample taken from deck
130						135'—deflector dislodged;
	14 (135)				135–152'—sandy interval	sample taken from deck
140						
	15 (143)	3:17pm				

Project: 2012 WADGER Geothermal Drilling Project location: Upper Wind River Valley Project number: 26L-RVS	Log of boring WRV-1 Sheet 3 of 5

WASHINGTON STATE DEPARTMENT OF Natural Resources	Logged by: J. Bowman	Drill start date: 8/6/2012
	Checked by: J. Czajkowski	Drill end date: 8/27/2012
Total depth of borehole (ft): 286.5	Borehole diameter (in.): 10"/8"6"	Drilling method: air rotary/casing advance
Approximate surface elevation (ft): 1151	Sampling method(s): grab	Drilling contractor: Schneider Equipment & Drilling Services
Groundwater depth (ft): 26	Legal location description: SE¼NE¼ sec.31 T05N R07E	

Depth (ft)	Sample ID (ft)	Time	Drill rate (ft/min)	Rock type	Material description	Remarks
		5:04pm	0.5			
		5:13pm				
150		8/16/12 10:00am	0.2		152–165'—sand with small amounts of pea gravel	
160	16 (160)	11:00am				
		11:50am	0.4		165–186'—sand with abundant gravel and dark gray (N3) broken pieces of medium-grained sandstone	
170						
180	17 (180)					
		12:40pm				
	18 (186)	2:15pm	1.11		186–220'—OHANAPECOSH FORMATION; dark gray (N3), fine- to coarse-grained, very soft, well-sorted, thinly bedded, sandstone with siltstone interbeds; red, green, and orange grains present in coarse layers	
190						
	19 (197)					
200		2:33pm				
	20 (203)	4:44pm	0.5			203'—some sandy alluvium present in grab sample; believed to have come from material stuck in blooie line
210						
	21 (215)					
220		3:17pm				

Project:	2012 WADGER Geothermal Drilling
Project location:	Upper Wind River Valley
Project number:	26L-RVS
Log of boring	WRV-1
Sheet	4 of 5
Logged by:	J. Bowman
Checked by:	J. Czajkowski
Drill start date:	8/6/2012
Drill end date:	8/27/2012
Total depth of borehole (ft):	286.5
Borehole diameter (in.):	10"/8"6"
Drilling method:	air rotary/casing advance
Approximate surface elevation (ft):	1151
Sampling method(s):	grab
Drilling contractor:	Schneider Equipment & Drilling Services
Groundwater depth (ft):	26
Legal location description:	SE¼NE¼ sec.31 T05N R07E

Depth (ft)	Sample ID (ft)	Time	Drill rate (ft/min)	Rock type	Material description	Remarks
220			0.5		220–225'—soft	
	22 (225)	5:20pm				
		8/20/12 12:07pm				
230						
	23 (234)		0.3			234'—larger sandstone material came
						out of deflector top
	24 (240)					
240						
		1:10pm				
		2:25pm				245'—deflector dislodged
			0.19			
250		2:56pm				
		3:17pm				
	25 (256)		0.73			256'—air hammer not firing, hammer
						piston flooded with water
260						300 - 500 gal/min, making hole
	26 (262)	3:36pm				with air only, not drill bit
		5:04pm				
270	27 (272)		0.30			
		5:40pm				
		8/20/12 12:20pm				
280						
	28 (285)				285–300'—small gravel-sized pieces of tuff breccia	278'—stopped casing
			2.5			advance, began air rotary drilling
290						

Project: 2012 WADGER Geothermal Drilling Project location: Upper Wind River Valley Project number: 26L-RVS		Log of boring WRV-1 Sheet 5 of 5
WASHINGTON STATE DEPARTMENT OF Natural Resources	Logged by: J. Bowman	Drill start date: 8/6/2012
	Checked by: J. Czajkowski	Drill end date: 8/27/2012
Total depth of borehole (ft): 286.5	Borehole diameter (in.): 10"/8"6"	Drilling method: air rotary/casing advance
Approximate surface elevation (ft): 1151	Sampling method(s): grab	Drilling contractor: Schneider Equipment & Drilling Services
Groundwater depth (ft): 26	Legal location description: SE¼NE¼ sec.31 T05N R07E	

Depth (ft)	Sample ID (ft)	Time	Drill rate (ft/min)	Rock type	Material description	Remarks
300	29 (300)	12:40pm	2.5		300–310'—harder material, with more abundant fine-grained sandstone	
310	30 (310)	1:45pm	4.0		310–342'—very small fragments of tuff breccia	
320	31 (322)	1:50pm				322'—pieces of wood debris
330	32 (332)	2:01pm	3.33			
340	33 (342)	2:07pm				342'—terminated drilling
350						
360						
370						

Figure A2. Temperature-gradient well WRV-1 completion diagram and temperature gradient data.

Project: 2012 WADGER Geothermal Drilling
Project location: Upper Wind River Valley
Project number: 26L RVS

Well name: WRV-1
Geologist: J. Bowman

WASHINGTON STATE DEPARTMENT OF Natural Resources

Borehole diameter(s) (in.)–include depths:
16" to 52'; 8" to 286.5'
Inner casing diameter (in.)–include depths:
2" to 286.5'

Drill start date: 8/6/2012
Drill end date: 8/27/2012
Date installed: 8/27/2012

Total depth of borehole (ft): 286.5
Casing elevation (ft): 1151
Groundwater depth (ft): 26

Legal location description:
SE¼NE¼ sec. 31 T05N R07E

Drilling method: air rotary / casing advance
Drilling contractor: Schneider Drilling

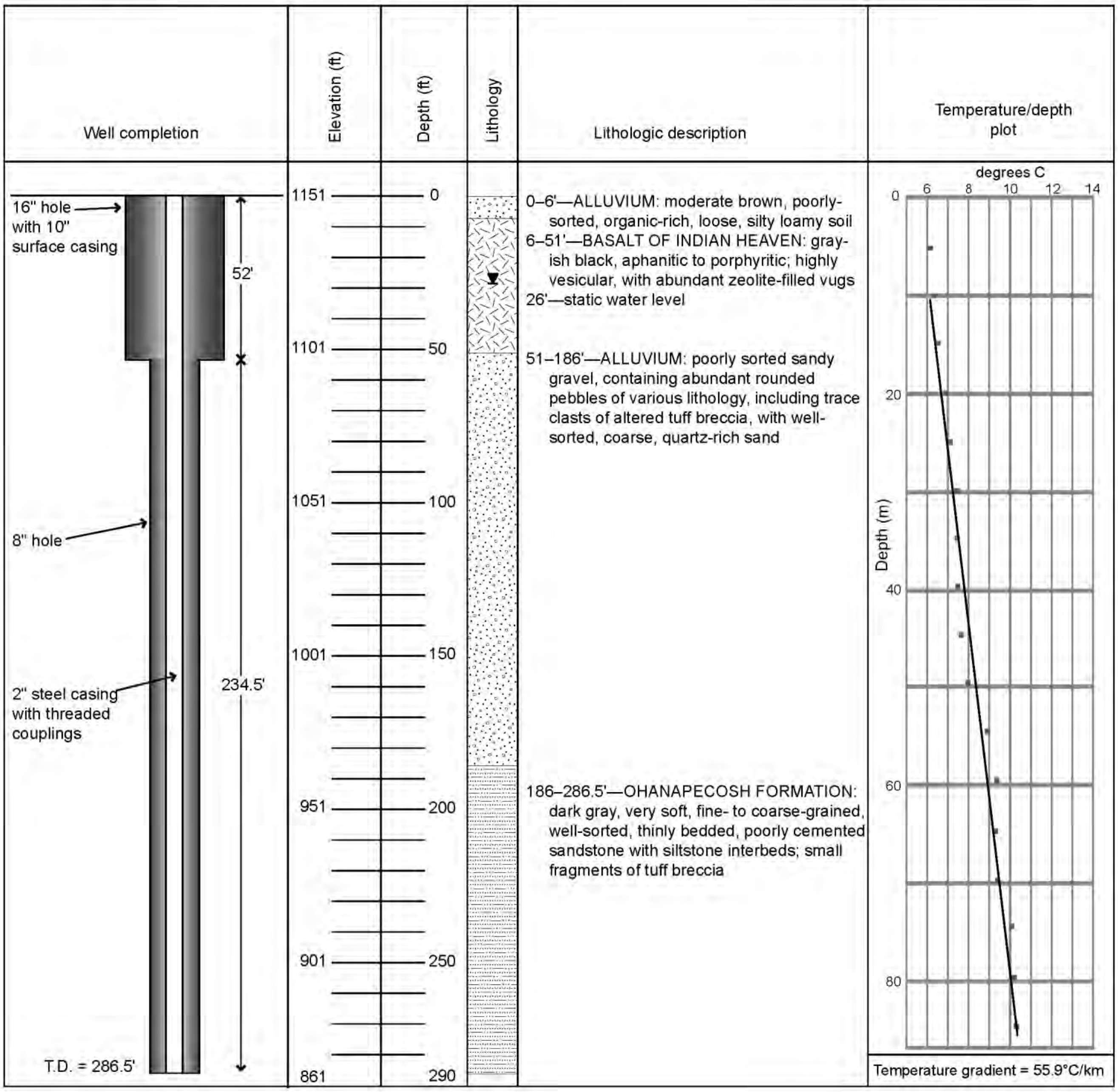

Figure A3. Temperature-gradient well WRV-1 geophysical log.

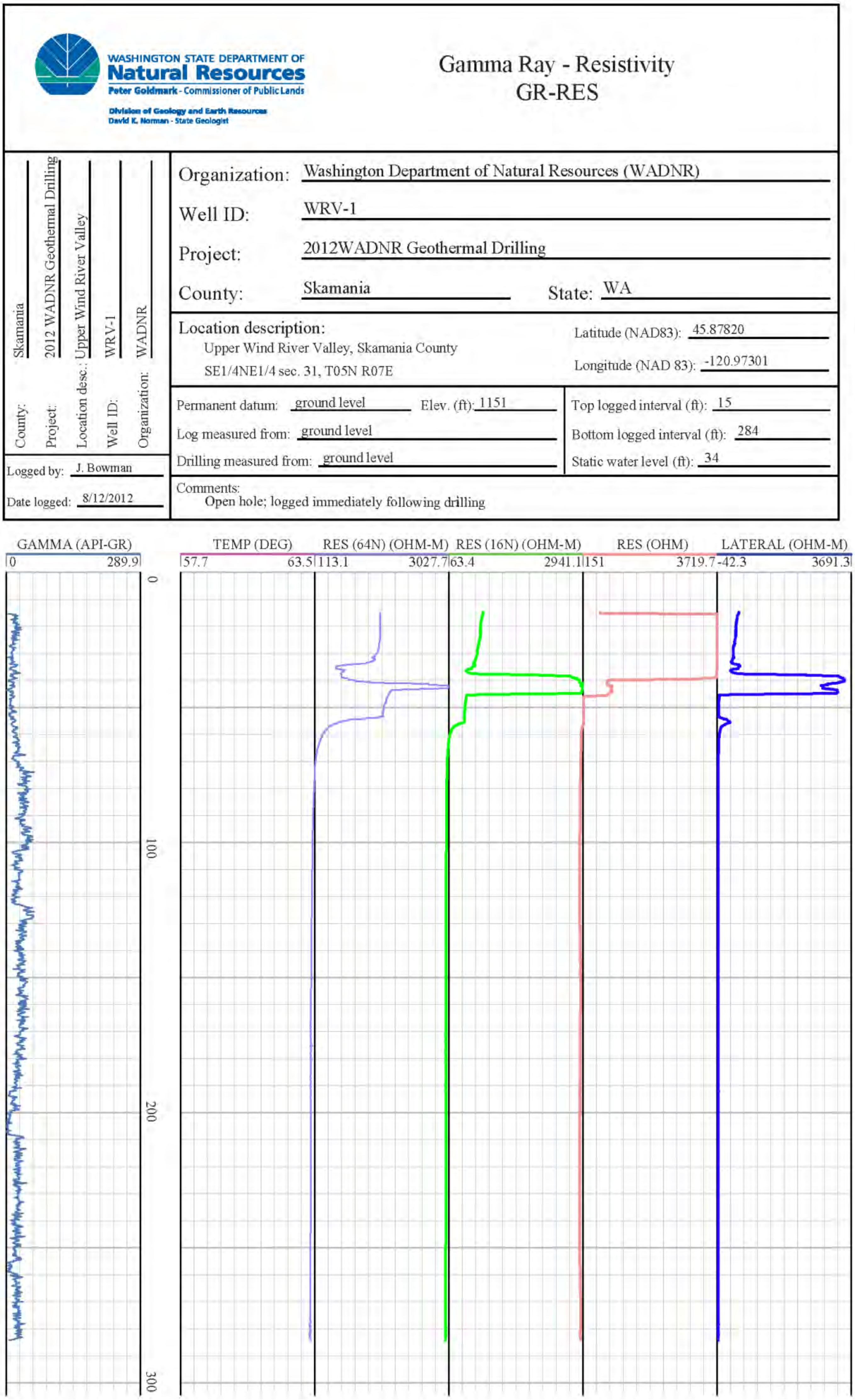

THIS PAGE INTENTIONALLY BLANK

Appendix B. Geophysical Survey Data

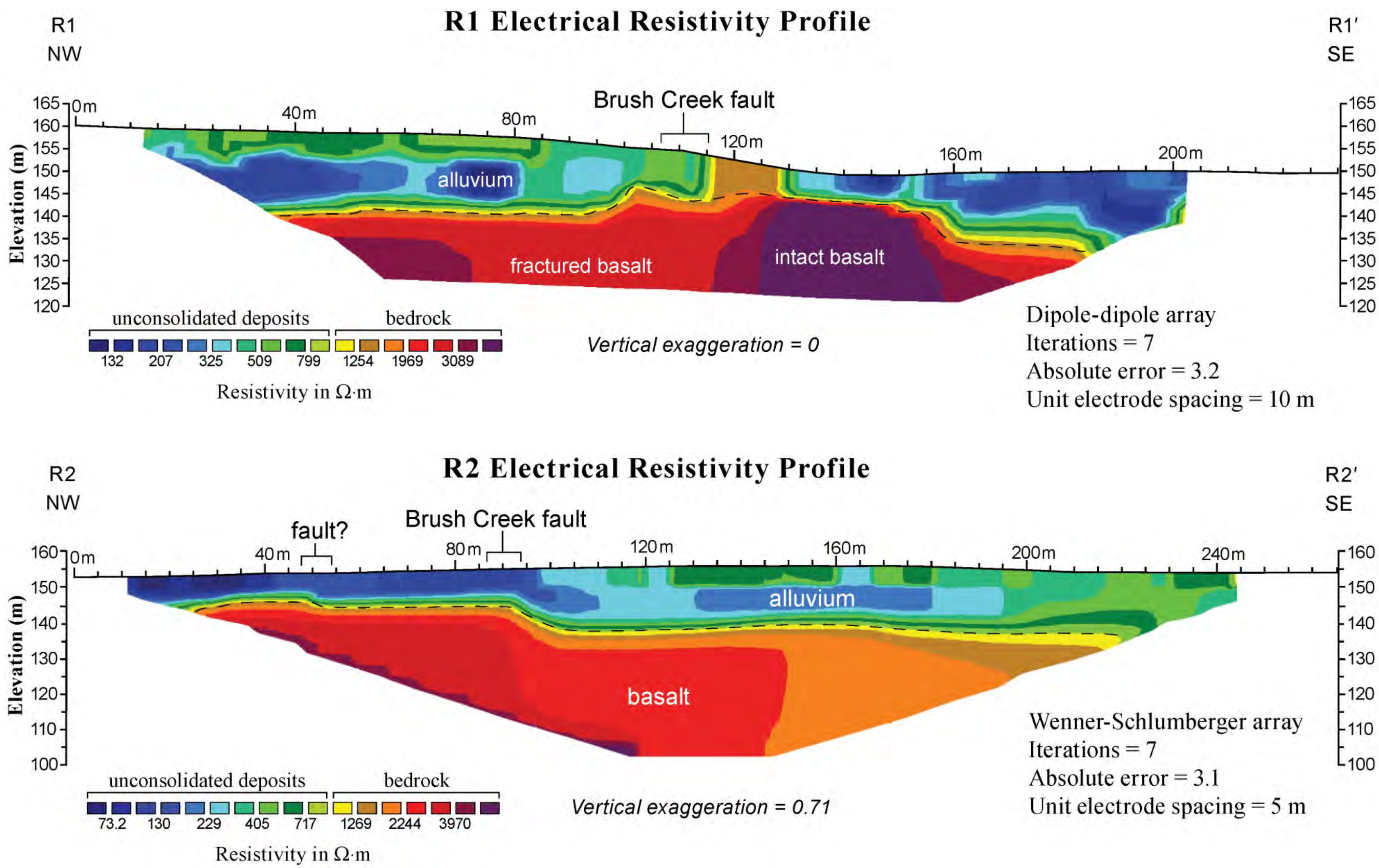

Figure B1. Electrical Resistivity profiles R1–R1′ and R2–R2′. Dashed black line denotes contact between basalt and overlying alluvium (not mapped).

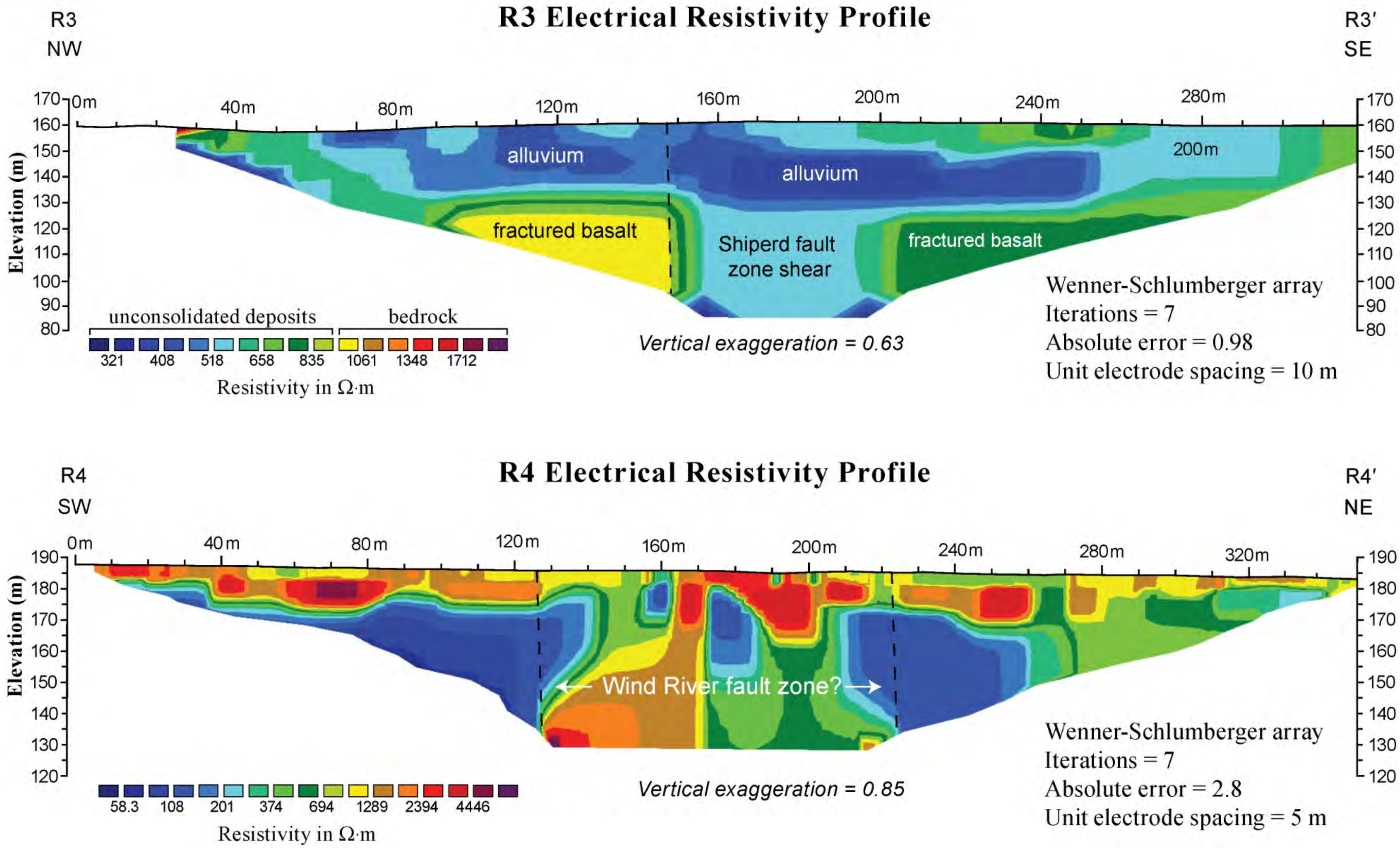

Figure B2. Electrical Resistivity profiles R3–R3′ and R4–R4′. Dashed black line denotes inferred fault contact.

WASHINGTON STATE DEPARTMENT OF
Natural Resources
Peter Goldmark - Commissioner of Public Lands

Division of Geology and Earth Resources
David K. Norman - State Geologist

WASHINGTON DIVISION OF GEOLOGY AND EARTH RESOURCES
OPEN FILE REPORT 2014-01
March 2014

Geologic Map and Geothermal Assessment of the Wind River Valley, Skamania County, Washington

Pamphlet accompanies map

Geologic Map and Geothermal Assessment of the Wind River Valley, Skamania County, Washington

by

Jessica L. Czajkowski, Jeffrey D. Bowman, Logan A. Fusso, and Darrick E. Boschmann

March 2014

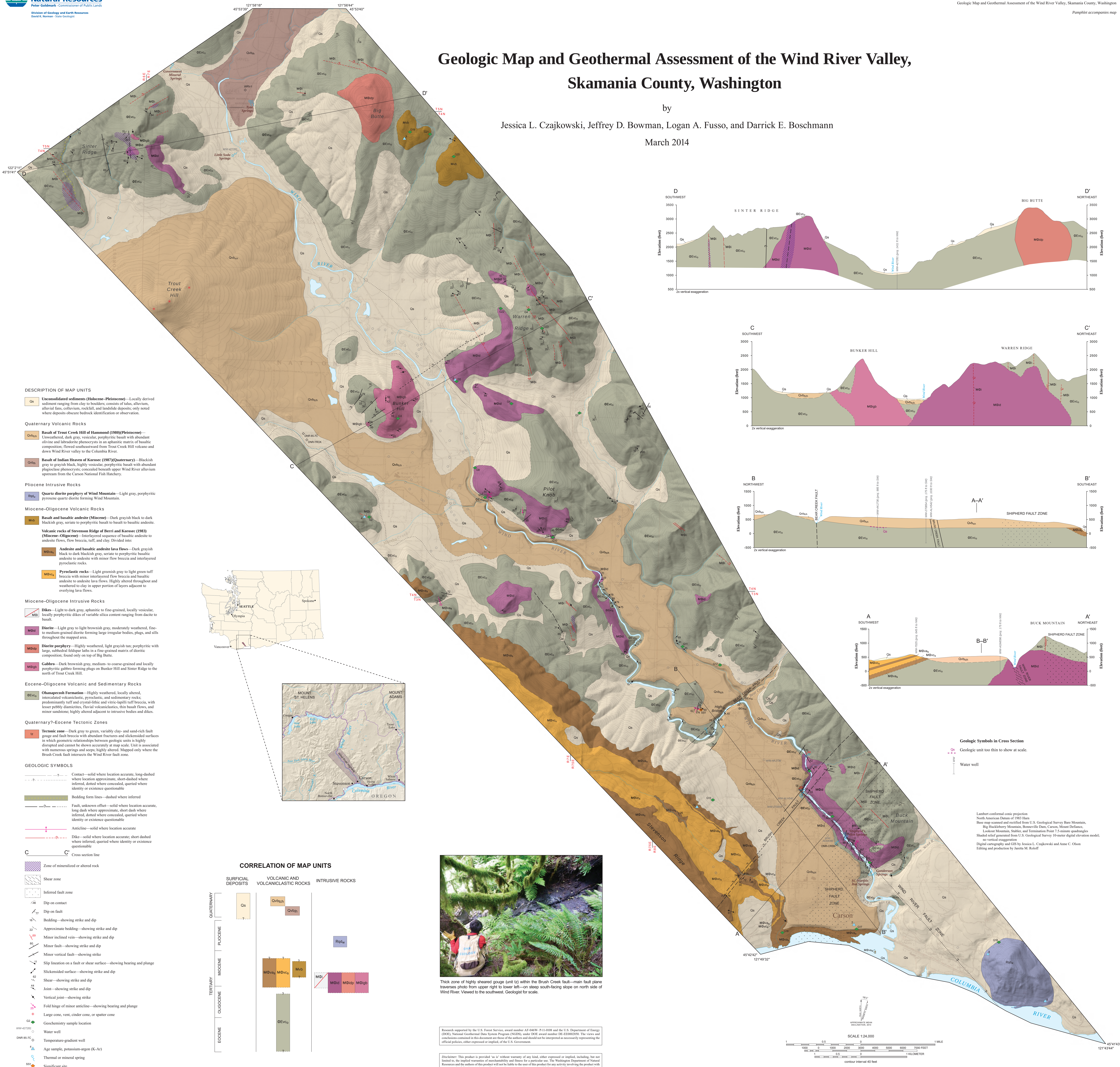

Geologic Symbols in Cross Section

Qs — Geologic unit too thin to show at scale.

WW — Water well

DESCRIPTION OF MAP UNITS

Qs — **Unconsolidated sediments (Holocene–Pleistocene)**—Locally derived sediment ranging from clay to boulders; consists of talus, alluvium, alluvial fans, colluvium, rockfall, and landslide deposits; only noted where deposits obscure bedrock identification or observation.

Quaternary Volcanic Rocks

$\mathrm{Qvb_{tch}}$ — **Basalt of Trout Creek Hill of Hammond (1980)(Pleistocene)**—Unweathered, dark gray, vesicular, porphyritic basalt with abundant olivine and labradorite phenocrysts in an aphanitic matrix of basaltic composition; flowed southeastward from Trout Creek Hill volcano and down Wind River valley to the Columbia River.

$\mathrm{Qvb_{ih}}$ — **Basalt of Indian Heaven of Korosec (1987)(Quaternary)**—Blackish gray to grayish black, highly vesicular, porphyritic basalt with abundant plagioclase phenocrysts; concealed beneath upper Wind River alluvium upstream from the Carson National Fish Hatchery.

Pliocene Intrusive Rocks

$\mathrm{Pqd_w}$ — **Quartz diorite porphyry of Wind Mountain**—Light gray, porphyritic pyroxene quartz diorite forming Wind Mountain.

Miocene–Oligocene Volcanic Rocks

Mvb — **Basalt and basaltic andesite (Miocene)**—Dark grayish black to dark blackish gray, seriate to porphyritic basalt to basalt to basaltic andesite.

Volcanic rocks of Stevenson Ridge of Berri and Korosec (1983) (Miocene–Oligocene)—Interlayered sequence of basaltic andesite to andesite flows, flow breccia, tuff, and clay. Divided into:

$\mathrm{M\Phi va_s}$ — **Andesite and basaltic andesite lava flows**—Dark grayish black to dark blackish gray, seriate to porphyritic basaltic andesite to andesite with minor flow breccia and interlayered pyroclastic rocks.

$\mathrm{M\Phi vc_s}$ — **Pyroclastic rocks**—Light greenish gray to light green tuff breccia with minor interlayered flow breccia and basaltic andesite to andesite lava flows. Highly altered throughout and weathered to clay in upper portion of layers adjacent to overlying lava flows.

Miocene–Oligocene Intrusive Rocks

$\mathrm{M\Phi i}$ — **Dikes**—Light to dark gray, aphanitic to fine-grained, locally vesicular, locally porphyritic dikes of variable silica content ranging from dacite to basalt.

$\mathrm{M\Phi id}$ — **Diorite**—Light gray to light brownish gray, moderately weathered, fine- to medium-grained diorite forming large irregular bodies, plugs, and sills throughout the mapped area.

$\mathrm{M\Phi idp}$ — **Diorite porphyry**—Highly weathered, light grayish tan; porphyritic with large, subhedral feldspar laths in a fine-grained matrix of dioritic composition; found only on top of Big Butte.

$\mathrm{M\Phi igb}$ — **Gabbro**—Dark brownish gray, medium- to coarse-grained and locally porphyritic gabbro forming plugs on Bunker Hill and Sinter Ridge to the north of Trout Creek Hill.

Eocene–Oligocene Volcanic and Sedimentary Rocks

$\mathrm{\Phi Evc_o}$ — **Ohanapecosh Formation**—Highly weathered, locally altered, intercalated volcaniclastic, pyroclastic, and sedimentary rocks; predominantly tuff and crystal-lithic and vitric-lapilli tuff breccia, with lesser pebbly diamictites, fluvial volcaniclastics, thin basalt flows, and minor sandstone; highly altered adjacent to intrusive bodies and dikes.

Quaternary?–Eocene Tectonic Zones

tz — **Tectonic zone**—Dark gray to green, variably clay- and sand-rich fault gouge and fault breccia with abundant fractures and slickensided surfaces in which geometric relationships between geologic units is highly disrupted and cannot be shown accurately at map scale. Unit is associated with numerous springs and seeps; highly altered. Mapped only where the Brush Creek fault intersects the Wind River fault zone.

GEOLOGIC SYMBOLS

Contact—solid where location accurate, long-dashed where location approximate, short-dashed where inferred, dotted where concealed, queried where identity or existence questionable

Bedding form lines—dashed where inferred

Fault, unknown offset—solid where location accurate, long dash where approximate, short dash where inferred, dotted where concealed, queried where identity or existence questionable

Anticline—solid where location accurate

Dike—solid where location accurate; short dashed where inferred; queried where identity or existence questionable

C — C' Cross section line

Zone of mineralized or altered rock

Shear zone

Inferred fault zone

46 Dip on contact

77 Dip on fault

16 Bedding—showing strike and dip

22 Approximate bedding—showing strike and dip

69 Minor inclined vein—showing strike and dip

80 Minor fault—showing strike and dip

Minor vertical fault—showing strike

11 Slip lineation on a fault or shear surface—showing bearing and plunge

Slickensided surface—showing strike and dip

62 Shear—showing strike and dip

44 Joint—showing strike and dip

Vertical joint—showing strike

25 Fold hinge of minor anticline—showing bearing and plunge

Large cone, vent, cinder cone, or spatter cone

G2 Geochemistry sample location

WW-427281 Water well

DNR 85-7C Temperature-gradient well

4 Age sample, potassium-argon (K-Ar)

Thermal or mineral spring

SS1 Significant site

CORRELATION OF MAP UNITS

	SURFICIAL DEPOSITS	VOLCANIC AND VOLCANICLASTIC ROCKS	INTRUSIVE ROCKS
QUATERNARY	Qs	Qvbtch, Qvbih	
TERTIARY — PLIOCENE			Pqdw
TERTIARY — MIOCENE		MΦvas, MΦvcs, Mvb	MΦi, MΦid, MΦidp, MΦigb
TERTIARY — OLIGOCENE		ΦEvco	
TERTIARY — EOCENE		ΦEvco	

Thick zone of highly sheared gouge (unit tz) within the Brush Creek fault—main fault plane traverses photo from upper right to lower left—on steep south-facing slope on north side of Wind River. Viewed to the southwest. Geologist for scale.

Research supported by the U.S. Forest Service, award number AF-046W- P-11-0108 and the U.S. Department of Energy (DOE), National Geothermal Data System Program (NGDS), under DOE award number DE-EE0002850. The views and conclusions contained in this document are those of the authors and should not be interpreted as necessarily representing the official policies, either expressed or implied, of the U.S. Government.

Lambert conformal conic projection
North American Datum of 1983 Harn
Base map scanned and rectified from U.S. Geological Survey Bare Mountain, Big Huckleberry Mountain, Bonneville Dam, Carson, Mount Defiance, Lookout Mountain, Stabler, and Termination Point 7.5-minute quadrangles
Shaded relief generated from U.S. Geological Survey 10-meter digital elevation model; no vertical exaggeration
Digital cartography and GIS by Jessica L. Czajkowski and Anne C. Olson
Editing and production by Jaretta M. Roloff